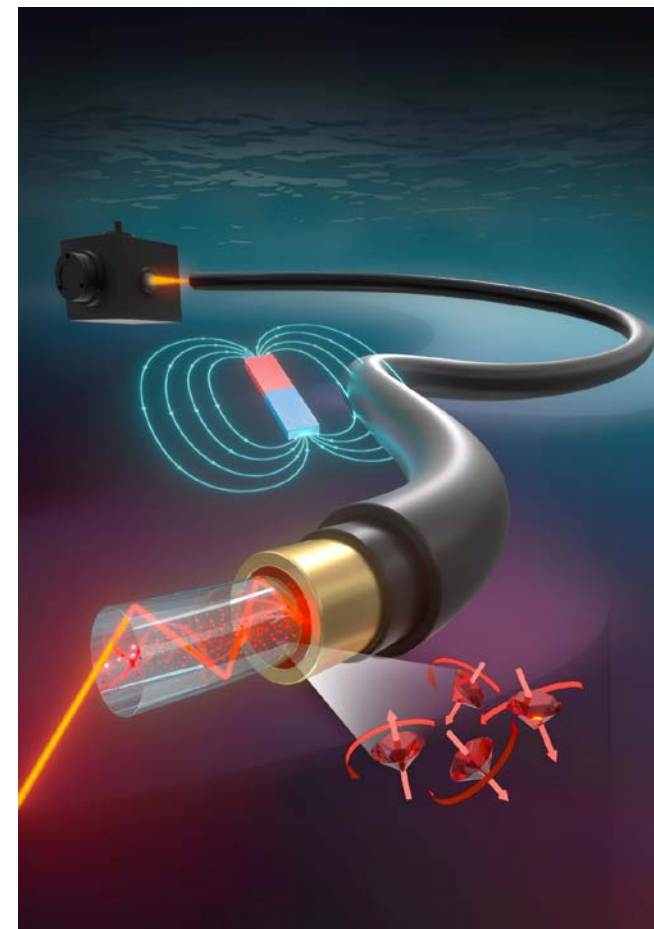


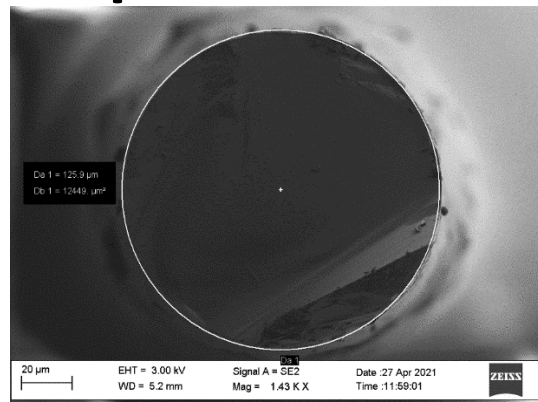
Volumetric integration of nanodiamonds in optical fiber cores

Ryszard Buczyński, Adam Filipkowski, Mariusz Mrózek, Grzegorz Stępniewski, Maciej Głowacki, Mateusz Ficek, Dariusz Pysz, Wojciech Gawlik, Robert Bogdanowicz, Adam Wojciechowski, Mariusz Klimczak

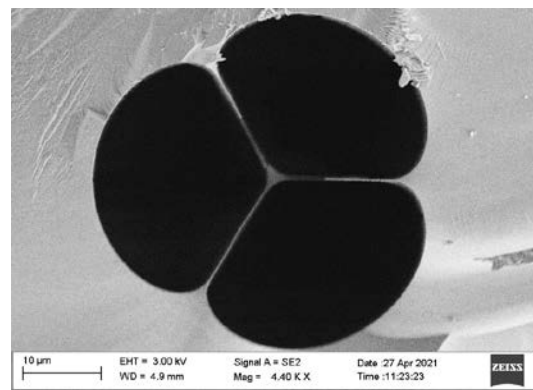


Agenda

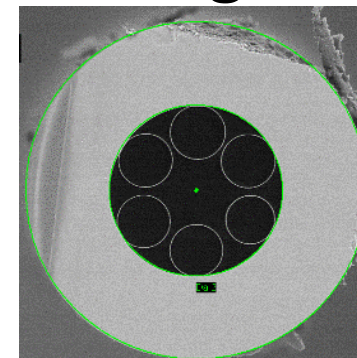
I. Optical fibers with with NV nanodiamonds: magnetometry



1. Step-index multimode fiber

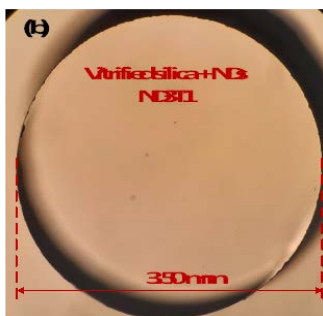


2. Step-index suspended core microstructured fiber

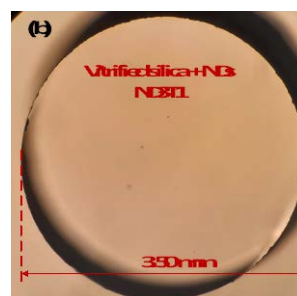


3. Hollow-core anti-resonant fiber

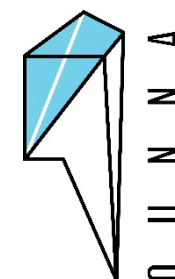
II. Optical fibers with nanodiamonds: reduction of nonlinearity



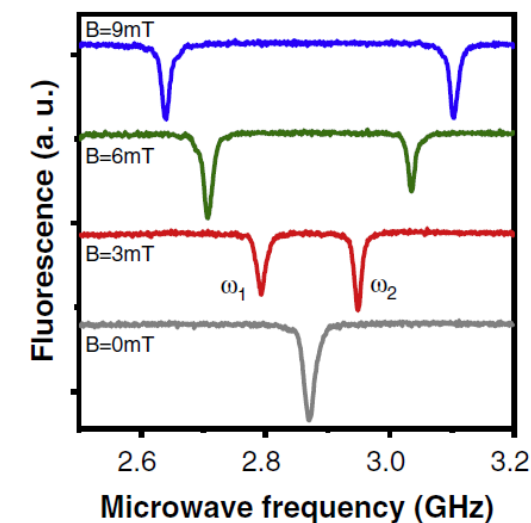
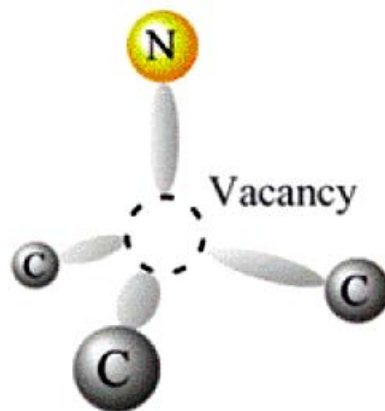
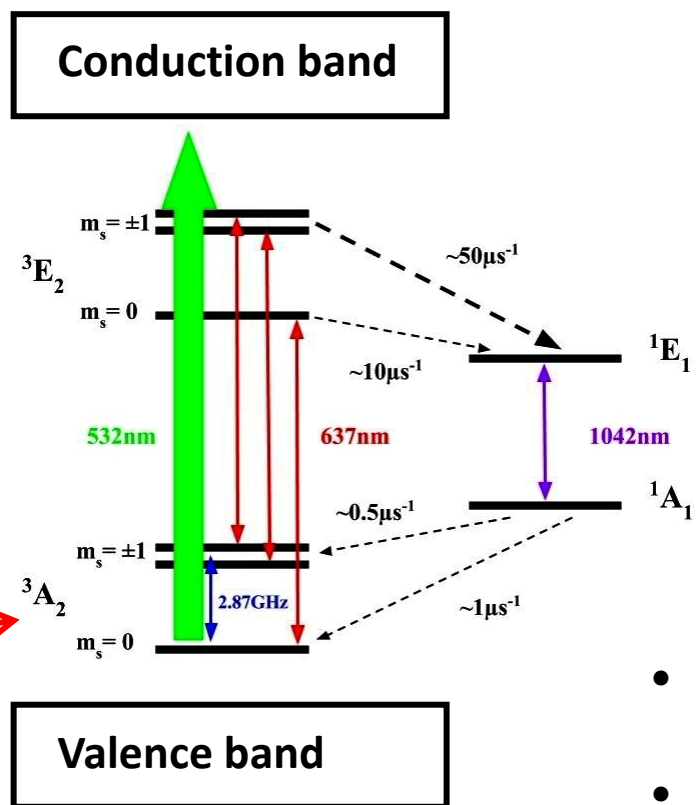
2. Step index fiber based on F2 glass with NDs



2. Vitrified silica glass with NDs

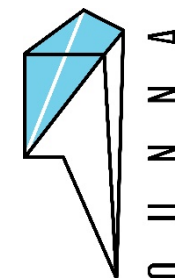


Magnetic field sensing with NV nanodiamonds



Spin polarization
of the ground state

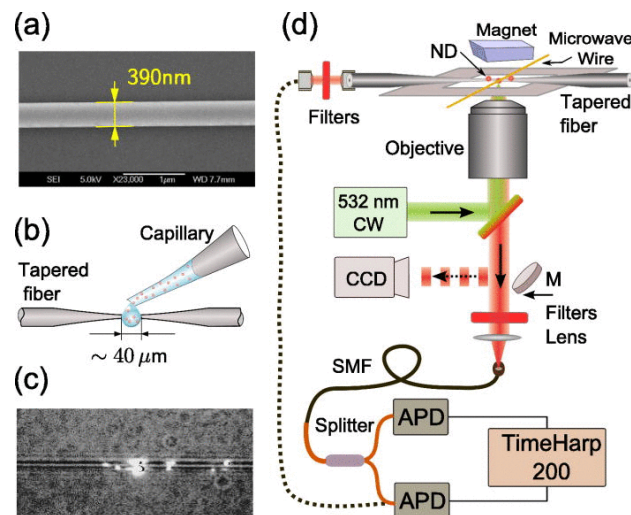
- Efficient fluorescence collection requires integration of NDs with specific platforms
- Optical pumping: population transfer from $|\pm 1\rangle$ to $|0\rangle$
- Optical readout: Optically Detected Magnetic Resonance (ODMR)
- **OPTICAL probing and readout of ND state can benefit from the integration with optical fibers**



Nanodiamond integration with optical fibers – the state of the art

Optical fiber tapers (evanescent field operation)

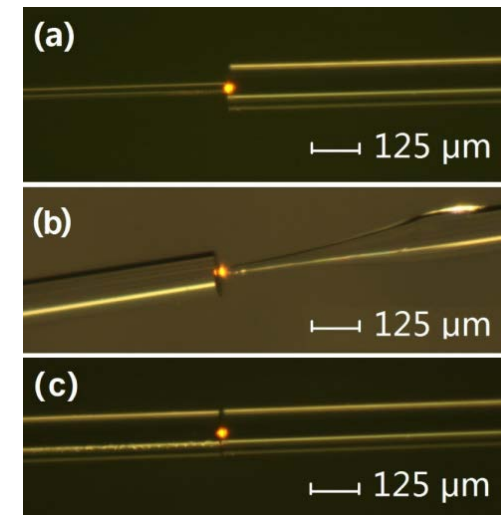
Xiaodi Liu et al. Appl. Phys. Lett. 103, 143105 (2013)



Fiber tip functionalization

T. Schröder et al. Optics Express 20, 10490 (2012)

D. Duan et al. Optics Express 27, 6734 (2019)



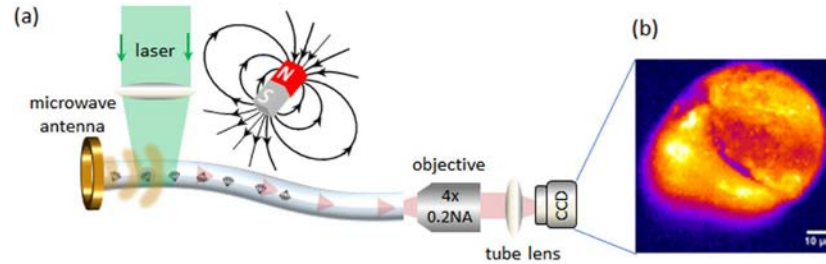
*Both approaches: ultra-precise, but highly localized
interaction with monitored object / field*

Diamond particle-doped glass & optical fiber

- *Doping* of diamond particles into glass and drawing into fibers:
magnetically sensitive optical fibers - 2014 & on: **prof. H. Ebendorff-Heidepriem & group, The University of Adelaide**

What for? + advantages

- Magnetically sensitive endoscopes for remote B-field sensing
- Immobilization and protection of diamonds
- Improvement of NV *fluorescence collection* efficiency



SCIENTIFIC REPORTS 2017

OPEN **Magnetically sensitive nanodiamond-doped tellurite glass fibers**

Received: 17 August 2017
Accepted: 22 December 2017
Published online: 19 January 2018

Yinlan Ruan¹, David A. Simpson², Jan Jeske¹, Heike Ebendorff-Heidepriem¹, Desmond W. M. Lau⁴, Hong Ji¹, Brett C. Johnson², Takeshi Ohshima³, Shahraam Afshar V.^{1,2}, Lloyd Hollenberg^{2,5}, Andrew D. Greentree⁴, Tanya M. Monro^{1,2} & Brant C. Gibson^{1*}

Limitations

- Survivability of diamonds at fiber-drawing temperatures
- Scattering loss at diamond particles



Solutions

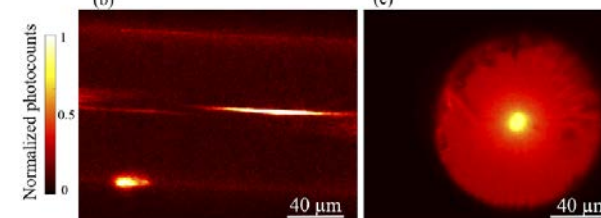
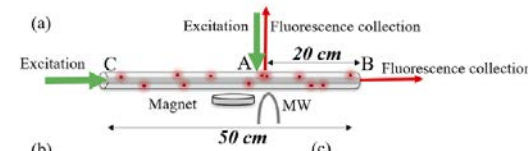
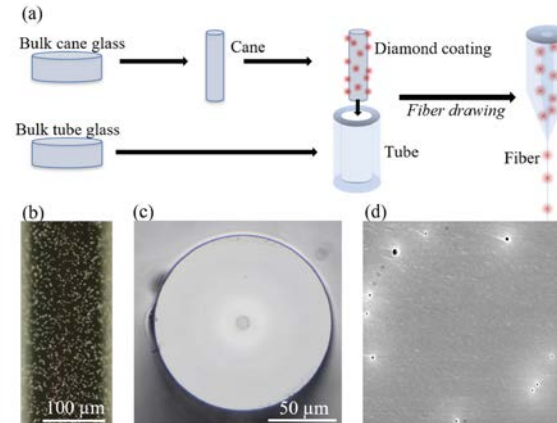
- Soft glasses drawable into fibers at 400-700 deg.C
- (i) Mixing diamonds into raw materials and melting glass - tellurite fibers
- (ii) Dip-coating preforms and drawing into fibers - lead-silicate glass fibers
- Structure modifications i.e. ring-shaped area of core doped with diamonds

Fluorescent diamond microparticle doped glass fiber for magnetic field sensing

Cite as: APL Mater. 8, 081102 (2020); <https://doi.org/10.1063/5.0013473>
Submitted: 12 May 2020 . Accepted: 21 July 2020 . Published Online: 03 August 2020

© D. Bai, M. H. Huynh, D. A. Simpson, P. Reineck, S. A. Vahid, A. D. Greentree, S. Foster, H. Ebendorff-Heidepriem, and B. C. Gibson

2020



Nanodiamond in tellurite glass Part II: practical nanodiamond-doped fibers

Yinlan Ruan,¹ Hong Ji,¹ Brett C. Johnson,² Takeshi Ohshima,³ Andrew D. Greentree,⁴ Brant C. Gibson,⁴ Tanya M. Monro¹ and Heike Ebendorff-Heidepriem^{1*}

2014

Results

- Guiding of NV fluorescence over fiber sections ~50 cm long
- < 1 μTVHz magnetic field sensitivity in ODMR measurements

Our approach

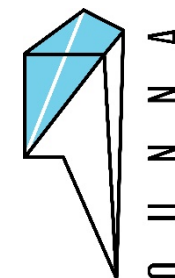
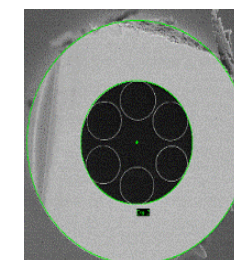
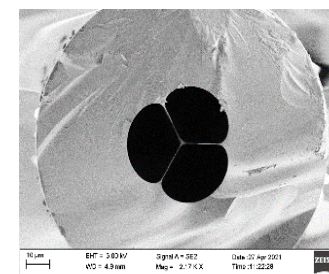
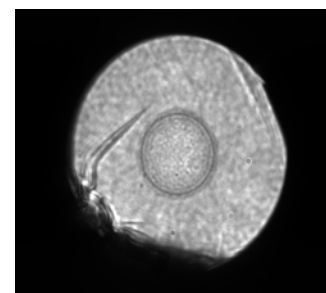
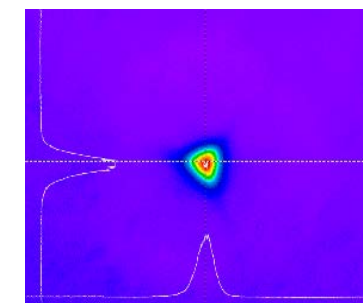
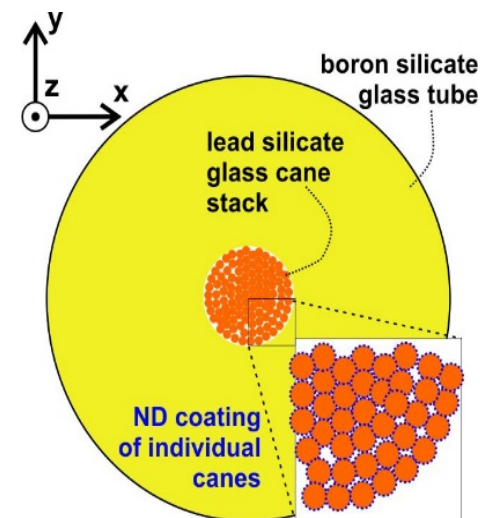
What do we do?

volumetric incorporation of NV diamonds in the fiber core

Why is it important?

- Enables scaling of concentration
- Enables distributed sensing
- Does not sacrifice magnetic response?

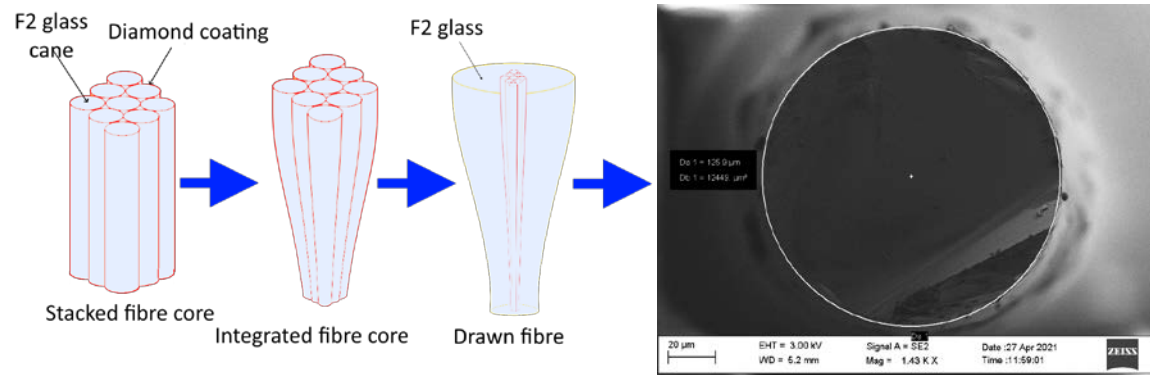
- Different fiber geometries enable addressing coupling efficiency of NV^- to guided modes



Our approach

How do we do it?

1. dip coating of glass preform components in ND liquid suspensions



Dip-coating of fiber preforms and drawing into fibers
- limited to single-ring topology

D. Bai et al., APL Mater. 8, 081102 (2020);

APL Materials

ARTICLE

scitation.org/journal/apm

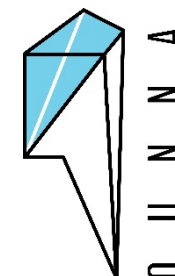
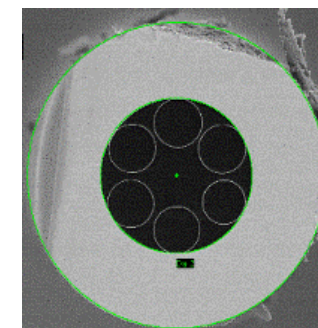
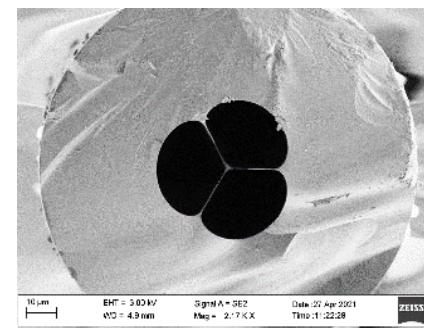
Fluorescent diamond microparticle doped glass fiber for magnetic field sensing

Cite as: APL Mater. 8, 081102 (2020); doi: 10.1063/5.0013473
Submitted: 12 May 2020 • Accepted: 21 July 2020 •
Published Online: 3 August 2020



D. Bai,¹ M. H. Huynh,² D. A. Simpson,³ P. Reineck,⁴ S. A. Vahid,⁵ A. D. Greentree,⁴ S. Foster,⁶ H. Ebendorff-Heidepriem,² and B. C. Gibson⁴

2. infiltration of hollow core fibers with ND liquid suspensions



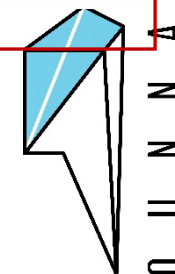
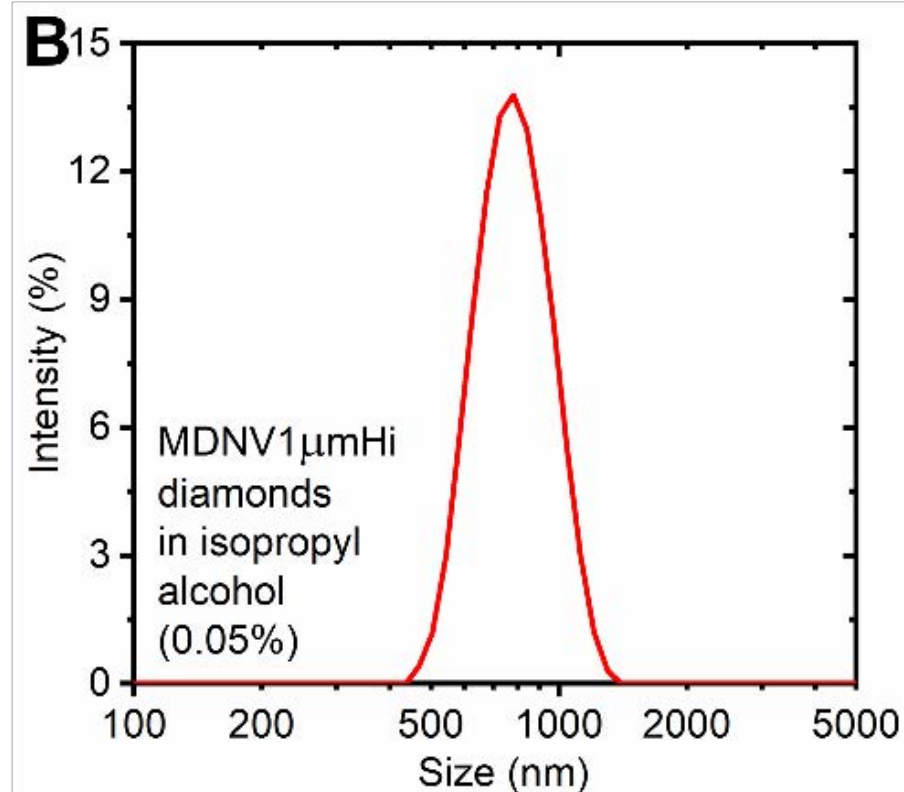
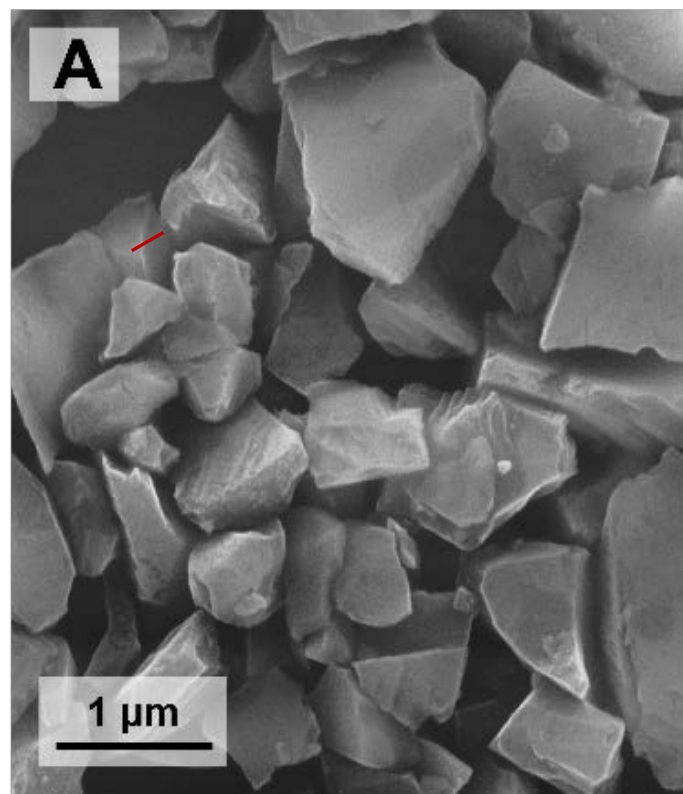
The ND deposited by infiltrating the core with IPA suspension followed by drying and flushing with pristine IPA.

Diamond particles for integration with glass

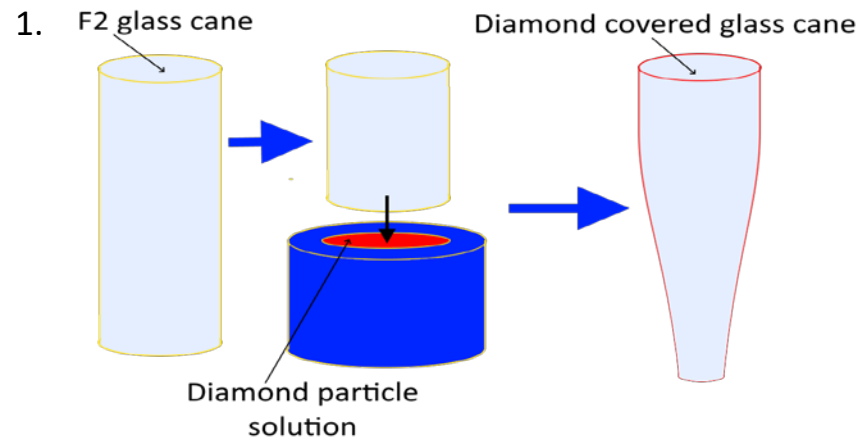
**MDNV1 μ m, Adámas
Nanotechnologies**

(developed using HPHT by
vendor)

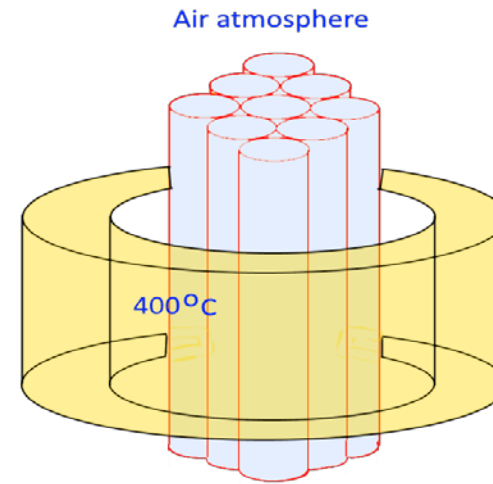
Mean particle size 750 nm
measured with the dynamic
light scattering method



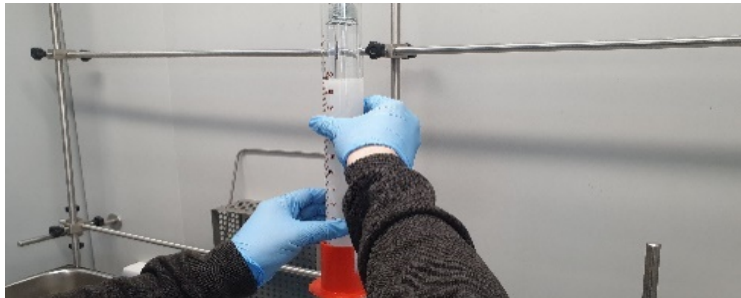
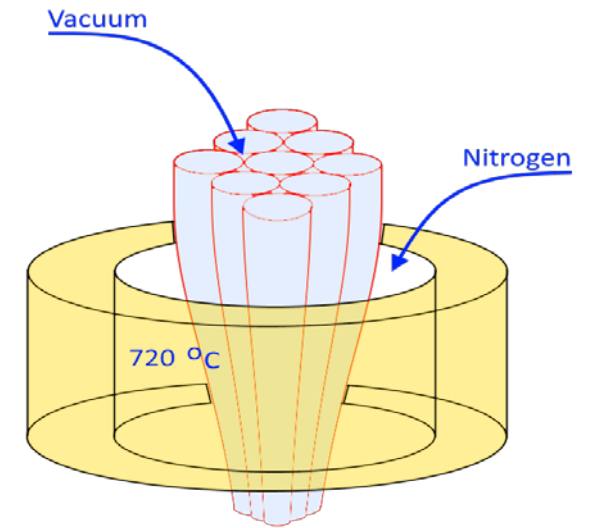
1. The step-index fiber



2.



3.

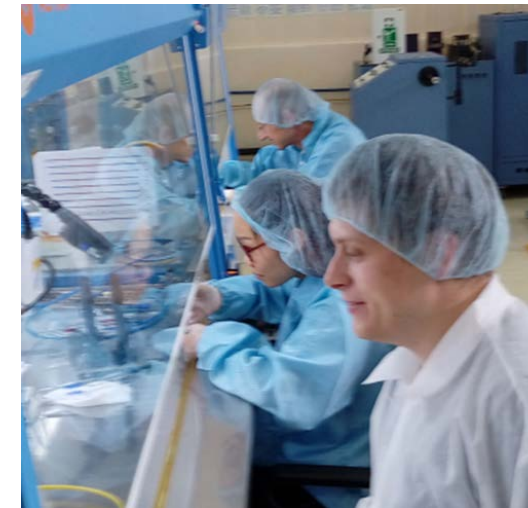


Nanodiamonds used:

- MDNV1um, Adámas Nanotechnologies ,
- NV concentration 3.5 ppm

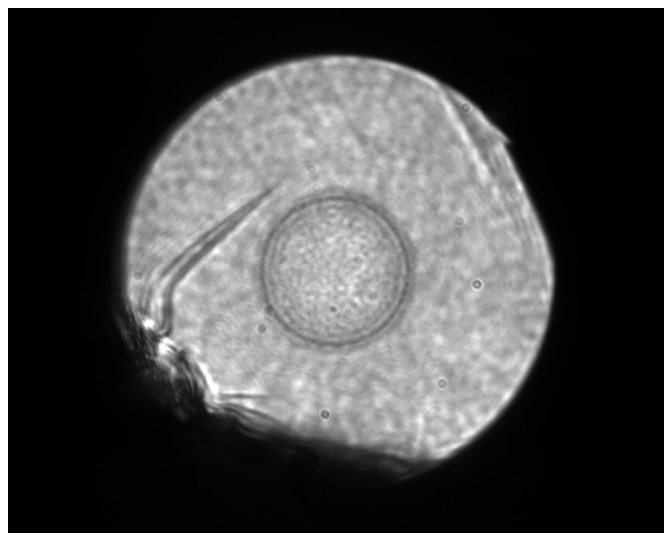
Fibre core:

- stacked using 790 glass rods
- coated with MD-NV-1um-Hi nanodiamonds 750 nm in size
- Schott F2 glass
- Low-index F2 modification for cladding tube

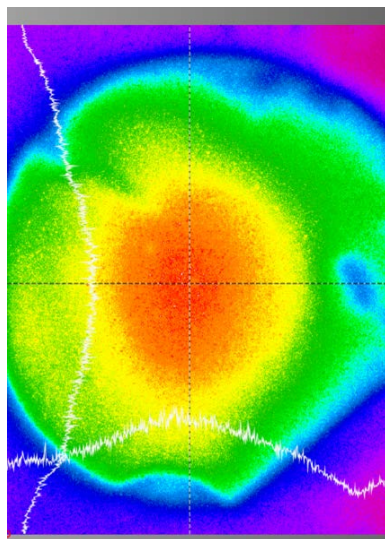


1. The step-index fiber

Cross-section of the fabricated fibre



Light intensity distribution for NV red fluorescence

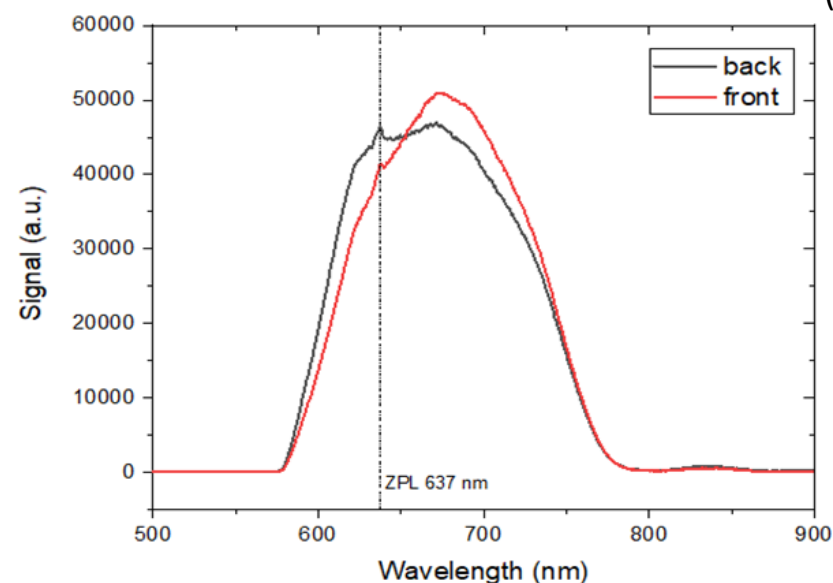


Fibre core:

- Core diameter 50 μm
- Schott F2 glass
- Low-index F2 modification for cladding tube
- Measured NA = 0.16

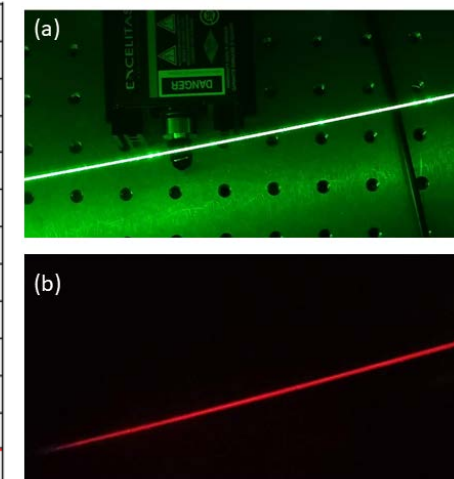
Fluorescence spectrum for:

- (a) excitation and detection from the same fibre end
(b) from different ends of the fiber

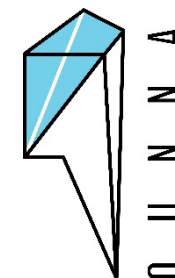


Light propagation in fibre

- (a) Without high pass filter
(b) With the filter



NV⁻ Zero phonon line at 637 nm visible
Asymmetry of spectra
Scattering observed



distribution of diamond particles at the glass surface

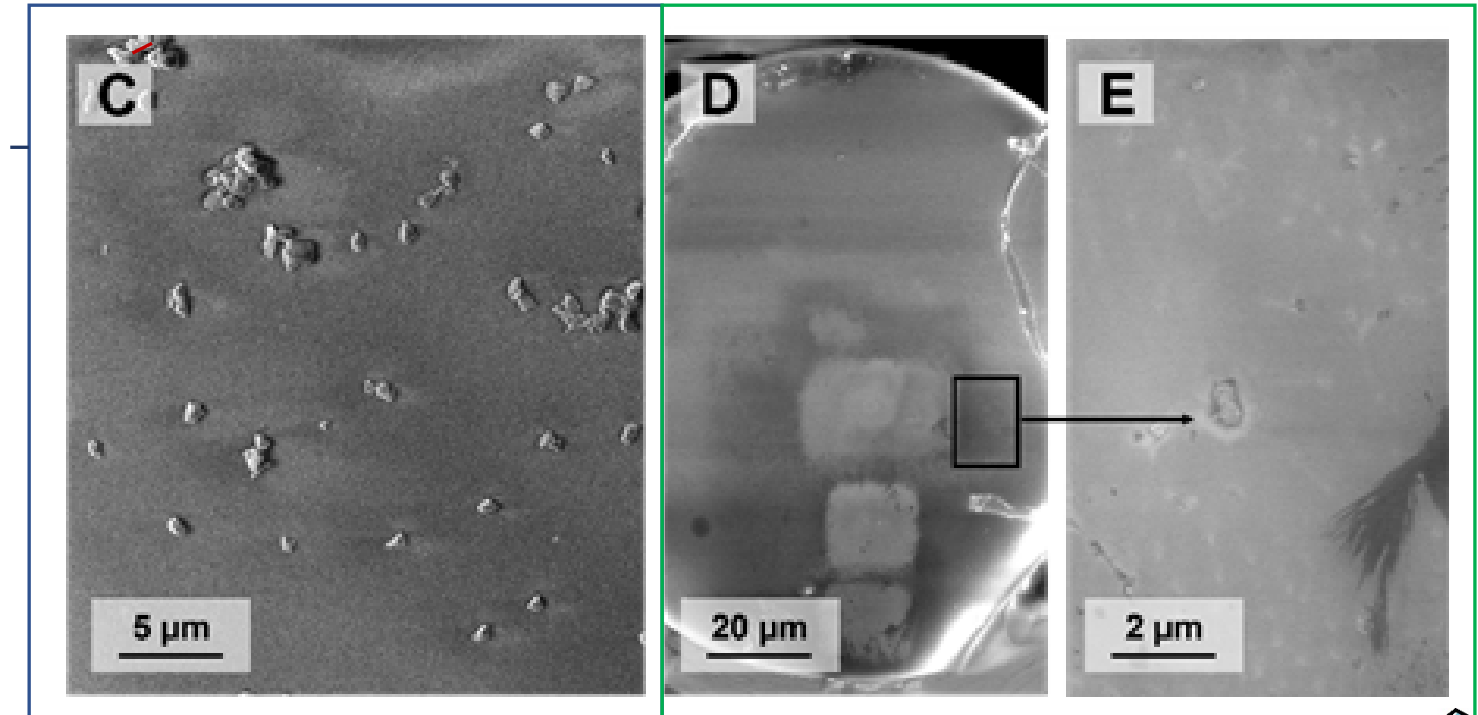
Surface of F2 silicate glass preform elements dip-coated with the nanodiamonds

No significant agglomeration

Typical particle-to-particle distance is between 2 μm and 5 μm

SEM images of fiber cross-section:

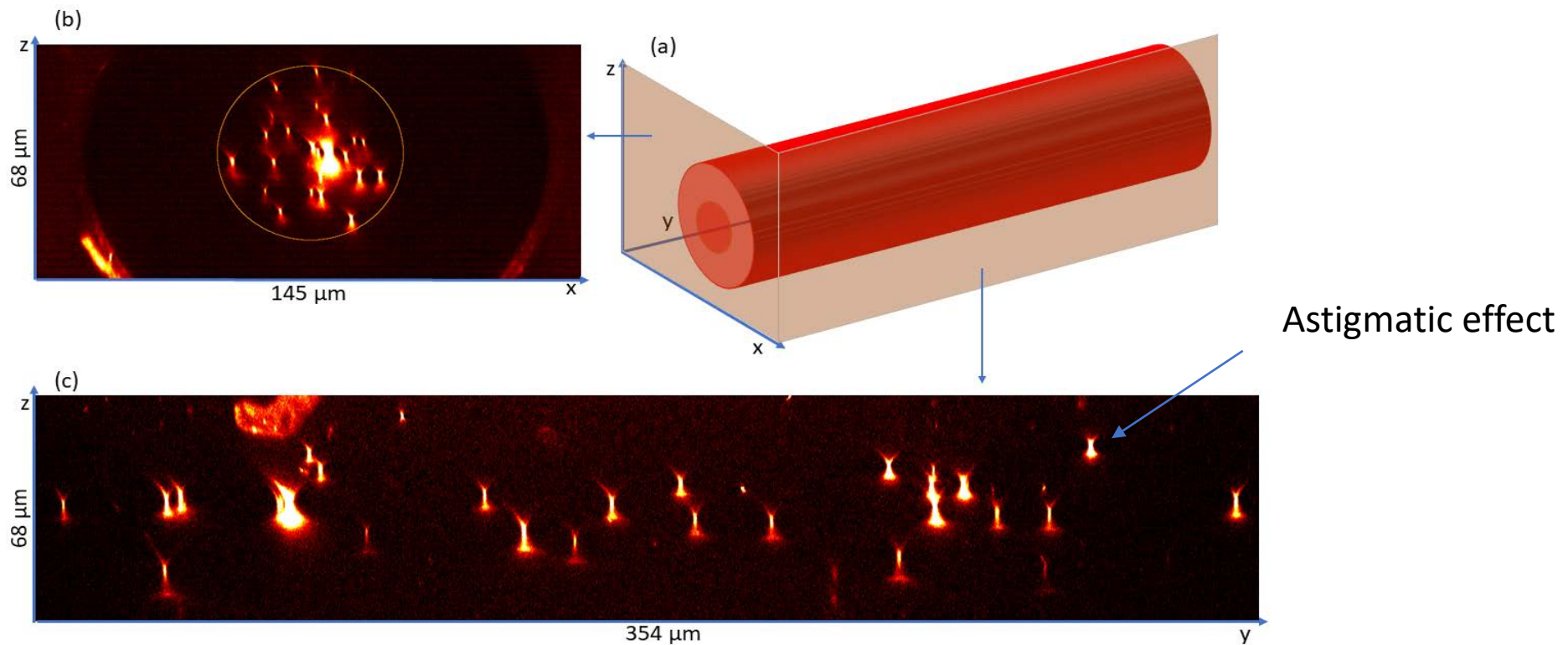
- homogenous glass structure with sectionally incorporated diamond particles
- no agglomerates
- no gass bubbles



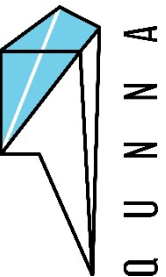
imaging of diamond particles distribution in the fiber core

Confocal microscopy imaging of ND distribution

- Observable fluorescence of individual NDs



- The method validates a reasonable degree of control over spatial ND distribution
- possible control of ND distribution by layout design

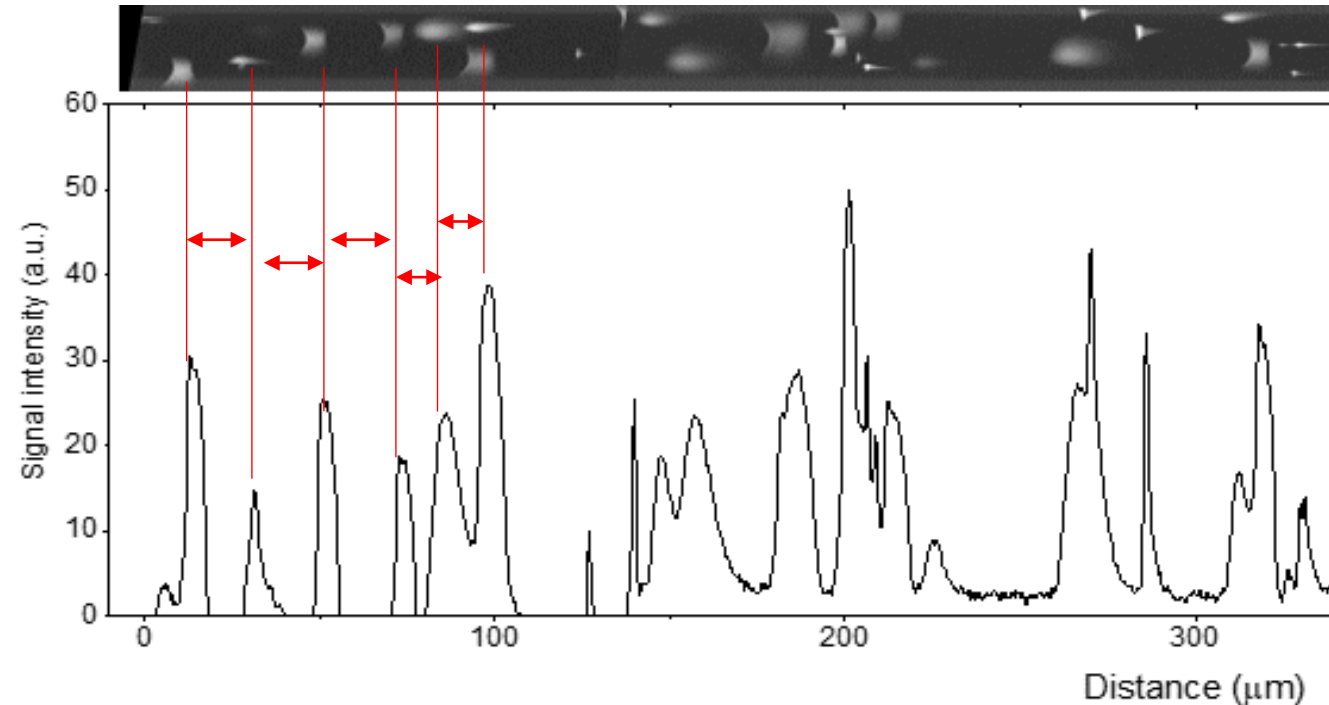


imaging of diamond particles distribution in the fiber core

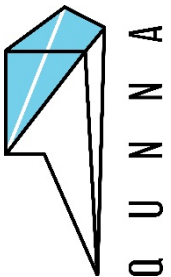
metodology

- recording of diamond fluorescence from either the face or the side of a fiber sample under a confocal microscope
- projecting the images from the 3 fiber samples (signal intensity) onto one axis,
- obtaining an intensity curve for either longitudinal or transverse axis of the fiber
- the distance between adjacent peaks is measured and obtained values are stacked in a histogram

Example of fiber image with fluorescing diamonds under a confocal microscope



Intensity curve from image projected onto fiber's longitudinal axis



imaging of diamond particles distribution in the fiber core

results

Longitudinal separation histogram:

major nanodiamond fractions

separated either by 15 μm or 25 μm

This corresponds to roughly 2.5 μm

diamond-diamond distance at

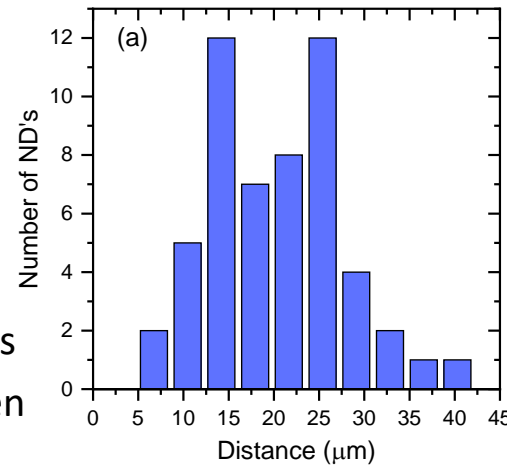
recorded at the dip-coated glass

surface, when fiber drawing dynamics

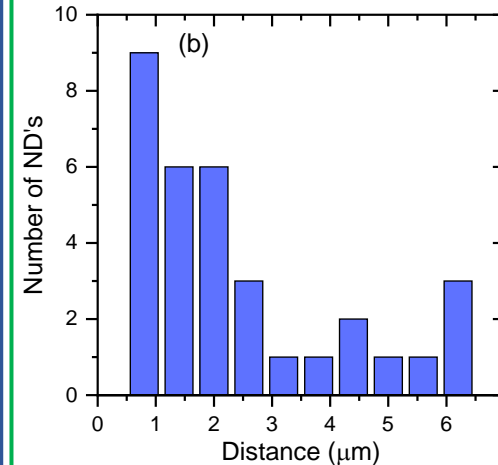
and drawing thin-down ratio are taken

into account.

Longitudinal plane



Transverse plane



Transverse separation histogram:

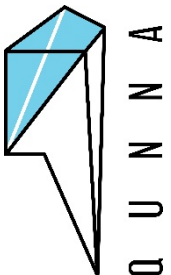
major fraction of NDs

separated 1-3 μm which

corresponds with mean cane

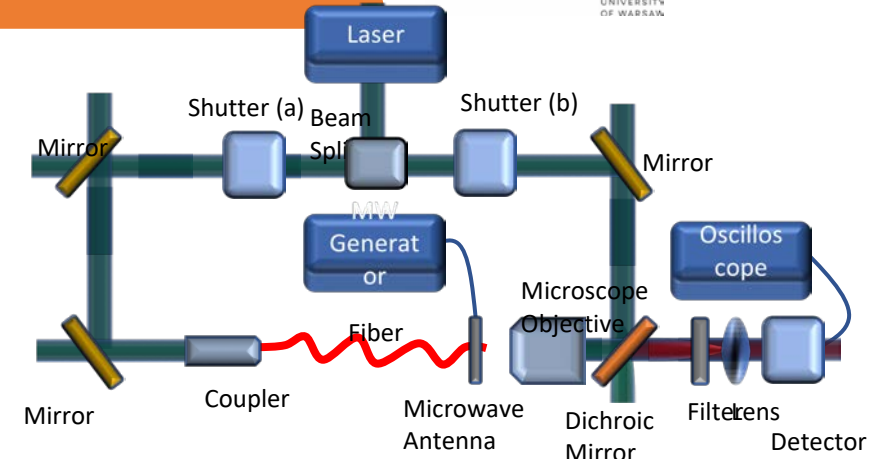
diameter in the final fiber core

(1.5 μm).



Magnetic field sensing performance

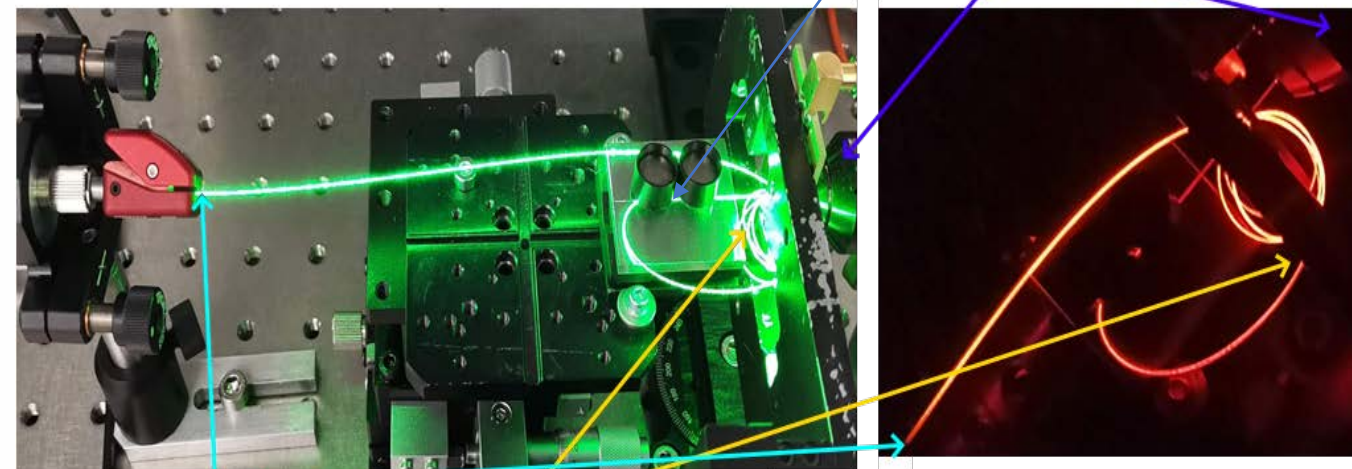
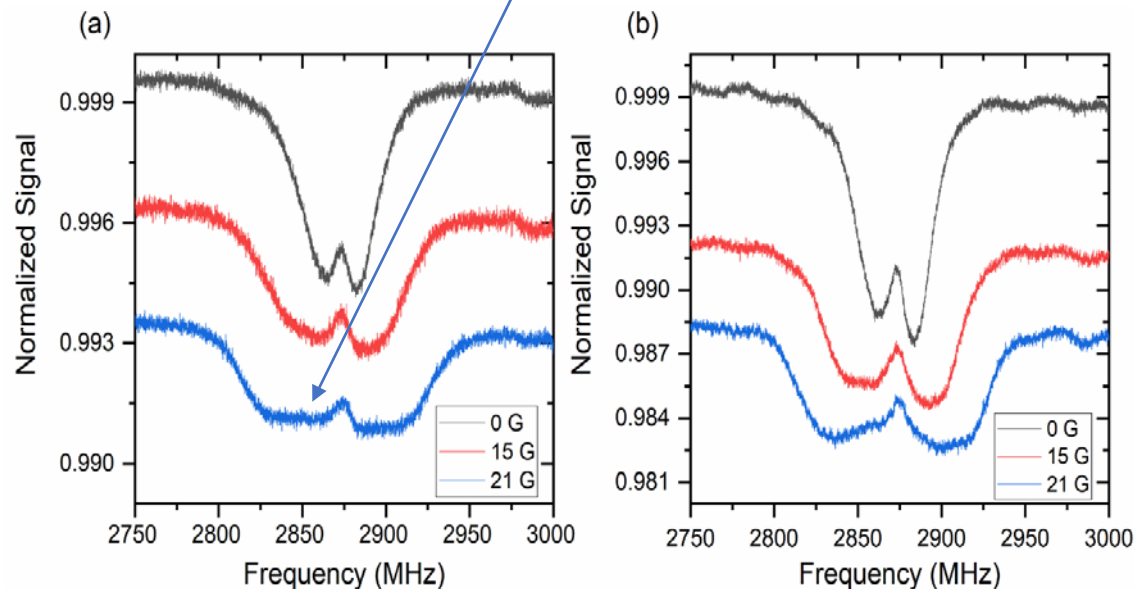
I. Proof of principle experiment: use of optically detected magnetic resonance (ODMR)



Continuous spectra – randomly oriented NDs

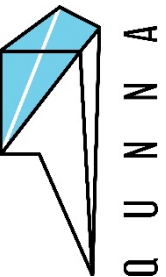
Fiber is looped around microwave antenna

Signal collection



Laser source

Microwave antenna



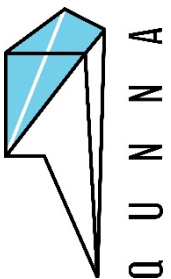
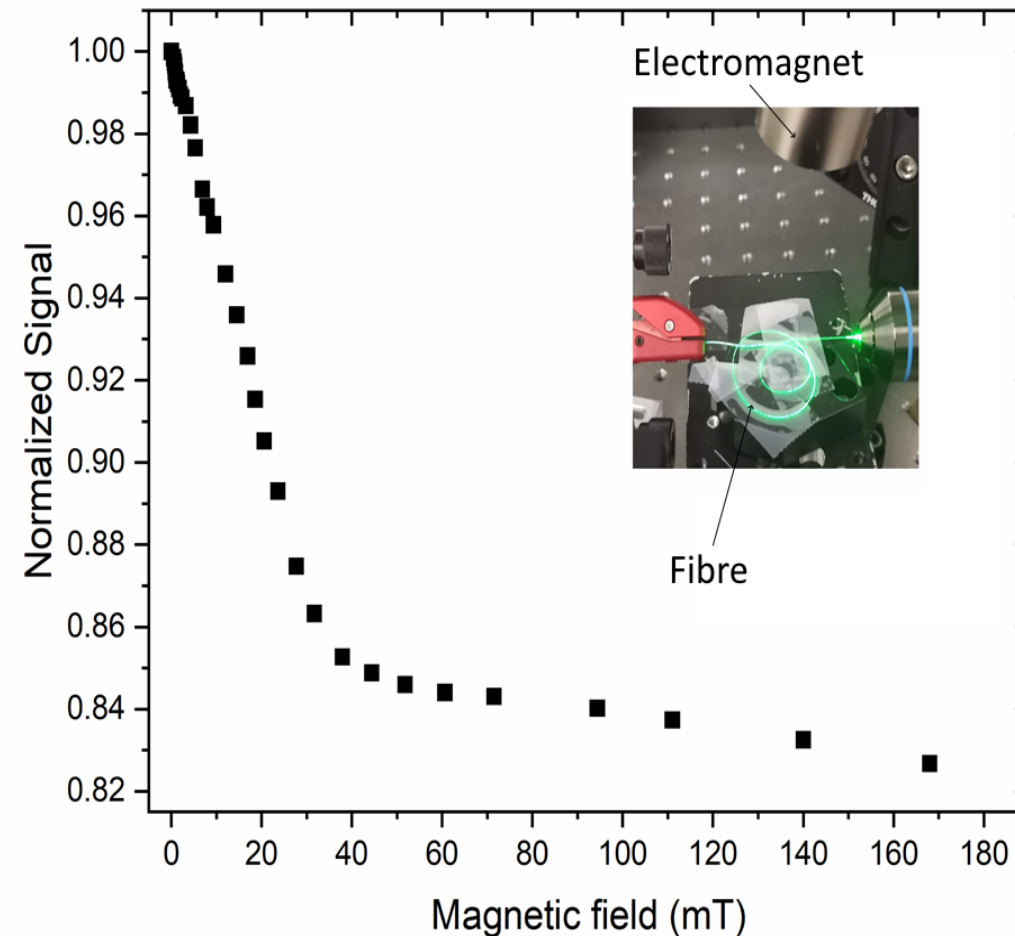
U N N A

- **Optically detected magnetic resonance measurements of fiber spun over a microwave antenna**
- **The read-out contrast between 0.5% to 1.3% - in both cases most of the fiber was not covered by the antenna (related to small fraction of fiber interacting with microwave)**

Magnetic field sensing performance

II. Direct magnetic field measurement - no microwaves

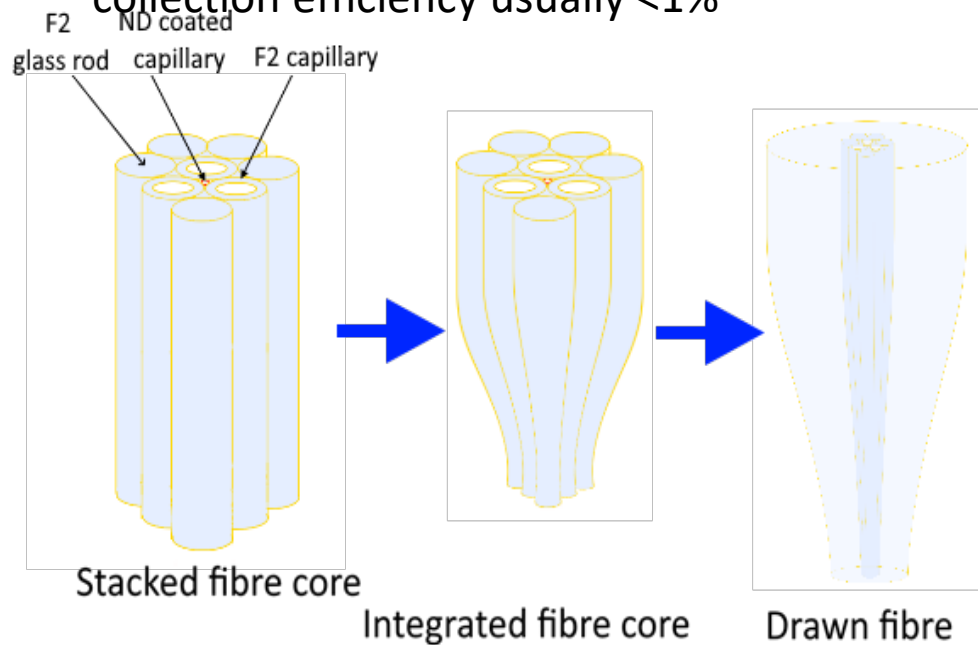
- Typical fluorescence decay curve observed
- 35 mT dynamics range, but low sensitivity
- (-) No microwaves - requires calibration for readout of magnetic field value
- (++) No microwaves - attractive for biosensing
- Only for high magnetic fields



2. The suspended core fiber

State of the art, comparable performance:

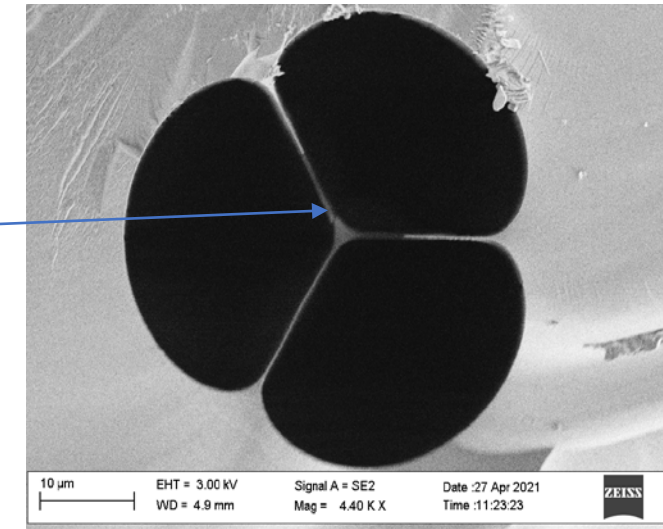
- fiber tip/taper magnetic field probes: tens of $\mu\text{T}/\sqrt{\text{Hz}}$ magnetic sensitivity & NV fluorescence collection efficiency usually $<1\%$



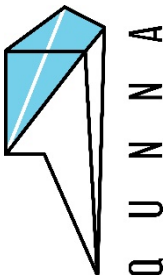
Core diameter 1.5
ND – 750 nm
Individual distribution of ND
along the fiber

What we do and why is it important:

- suspended core geometry: ND particles localized inside the volume and along the length of a 1.5 μm diam. core
- tight confinement of the guided mode and spatial overlap of NDs with the guided mode



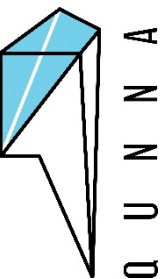
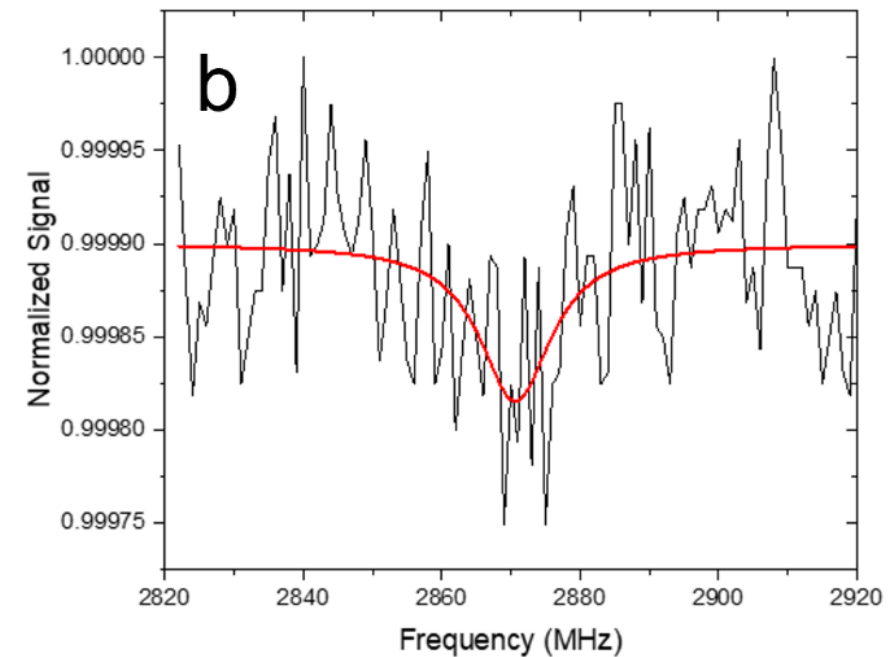
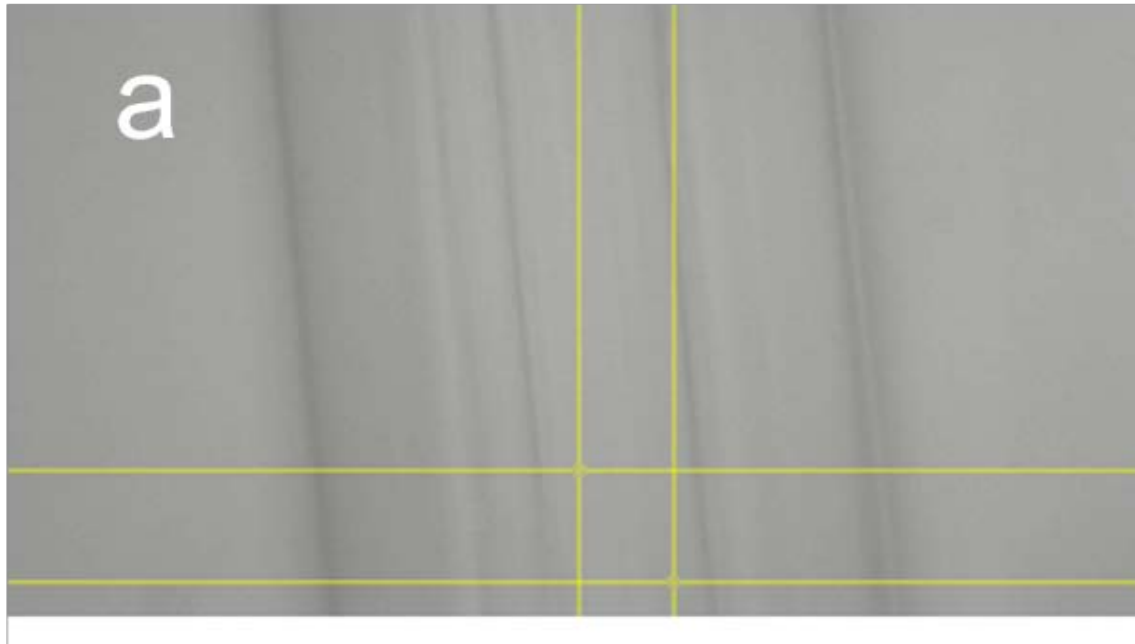
- The ND suspension introduced inside the glass tube and allowed to dry.
- The process repeated 10 times,
- avoiding wetting of the tube outside, to ensure even coating of nanodiamonds only at the inside surface of the glass tube
- Tube collapsed on fiber drawing tower



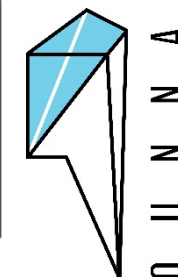
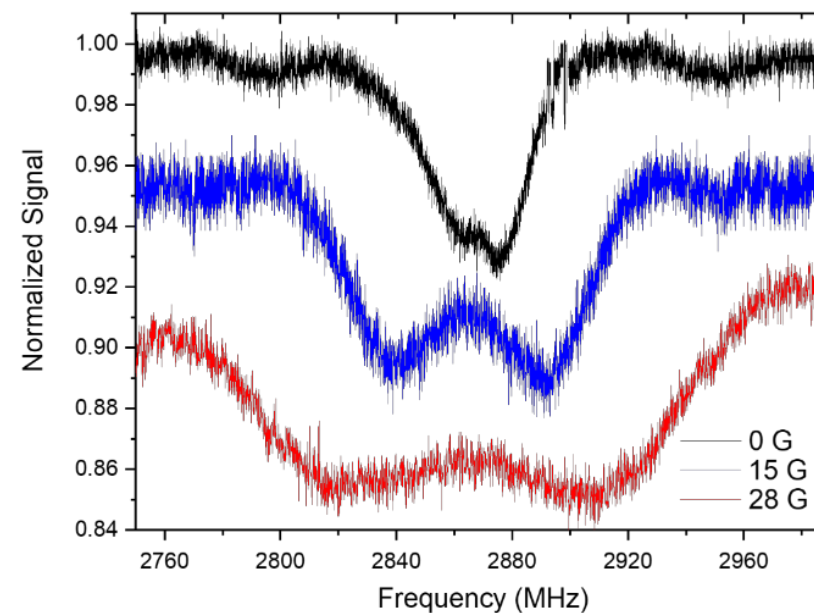
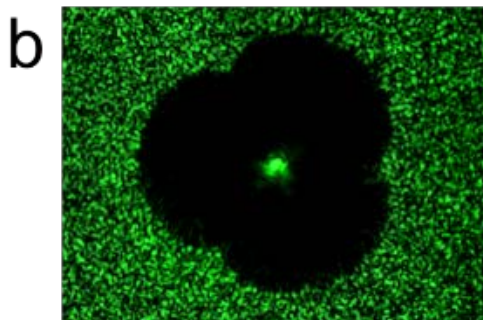
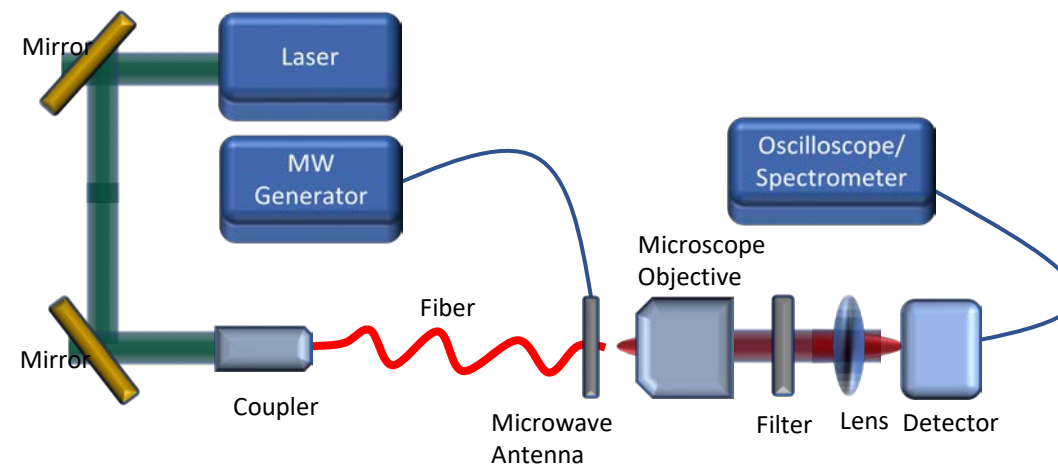
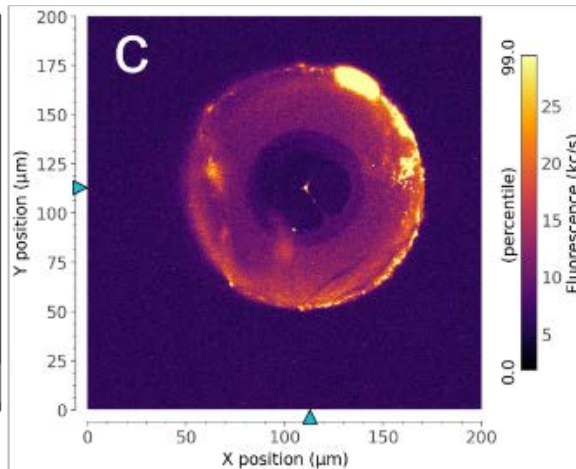
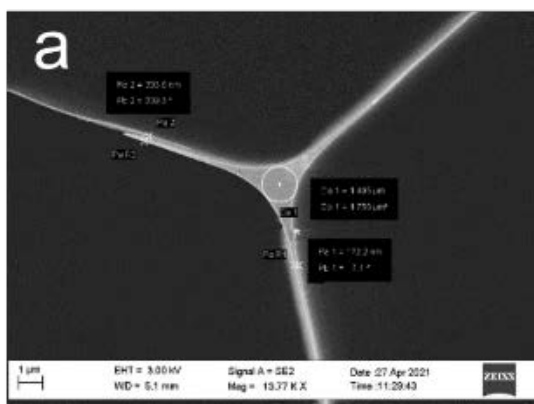
Magnetic field sensing performance

Side-mode operation verification

- Attempt to collect NV fluorescence from the fiber
- Hardly any fluorescence visible under the confocal microscope
- Error-bar level sensitivity :-)
- ✓ Supports strong confinement and guidance of NV fluorescence



Magnetic field sensing performance



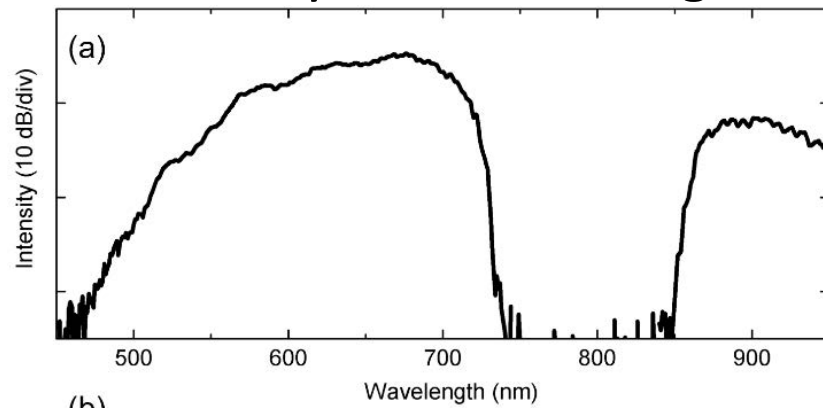
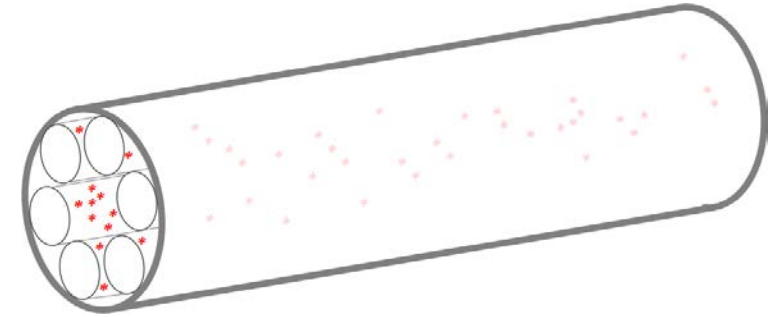
RESULTS:

- ✓ Magnetic sensitivity **500 nT/sqrt(Hz)**
- ✓ suspended core fiber 7% optical readout contrast in end-to-end ODMR
- ✓ („Transmission mode operation“)
- ✓ Strong confinement of NV fluorescence - strong **coupling**

3. Hollow-core anti-resonant fiber

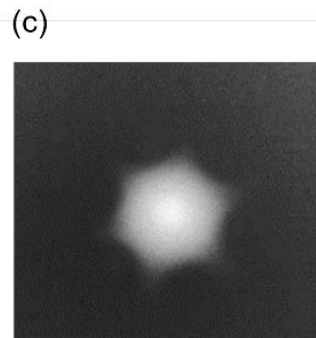
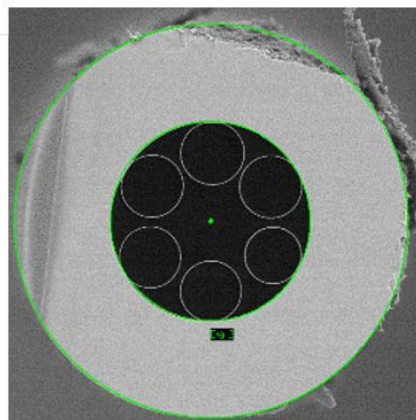
Why hollow core fiber?

- ✓ Largely unexplored in this application
- ✓ Coupling to guided mode difficult to anticipate
- ✓ Possible exposure of NDs to agents introduced into the hollow core
- ✓ Potentially low scattering loss



Hollow core fiber selection

- Silica, six non-touching capillaries in cladding
- 30 μm core diam.
- , 500 nm membrane thickness
- Broad VIS transmission covering both 532 nm excitation line and 637 nm NV⁻ Zero phonon line
- Effectively single mode at 637 nm

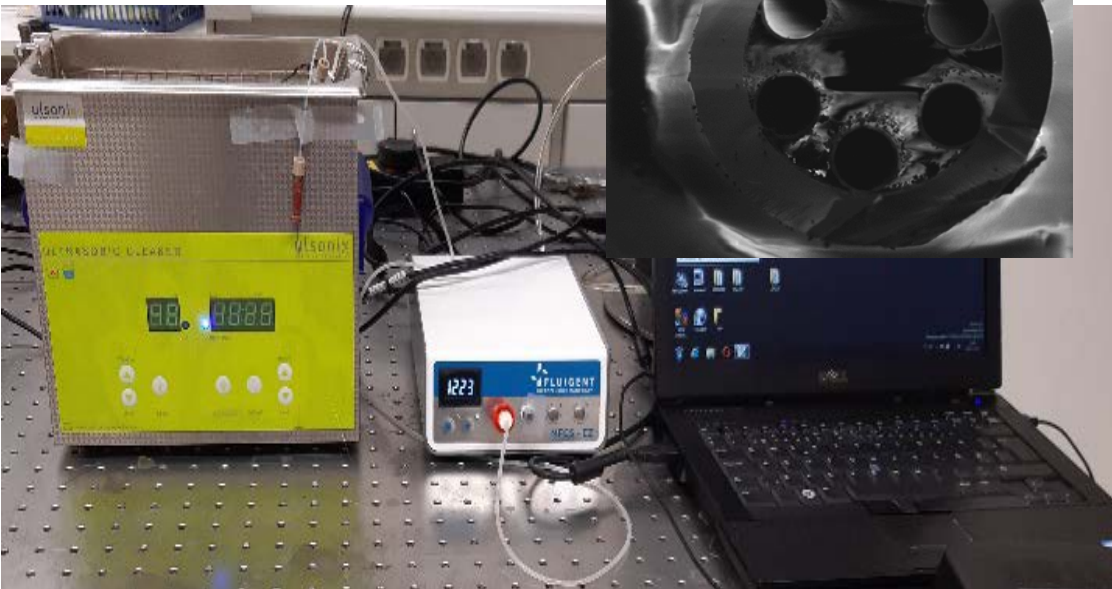
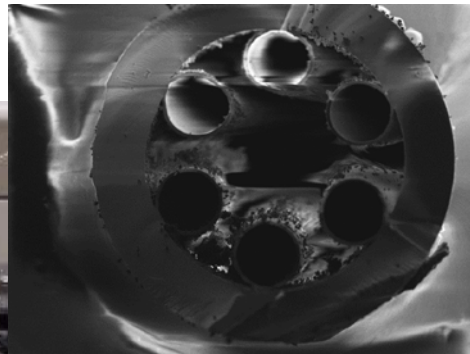
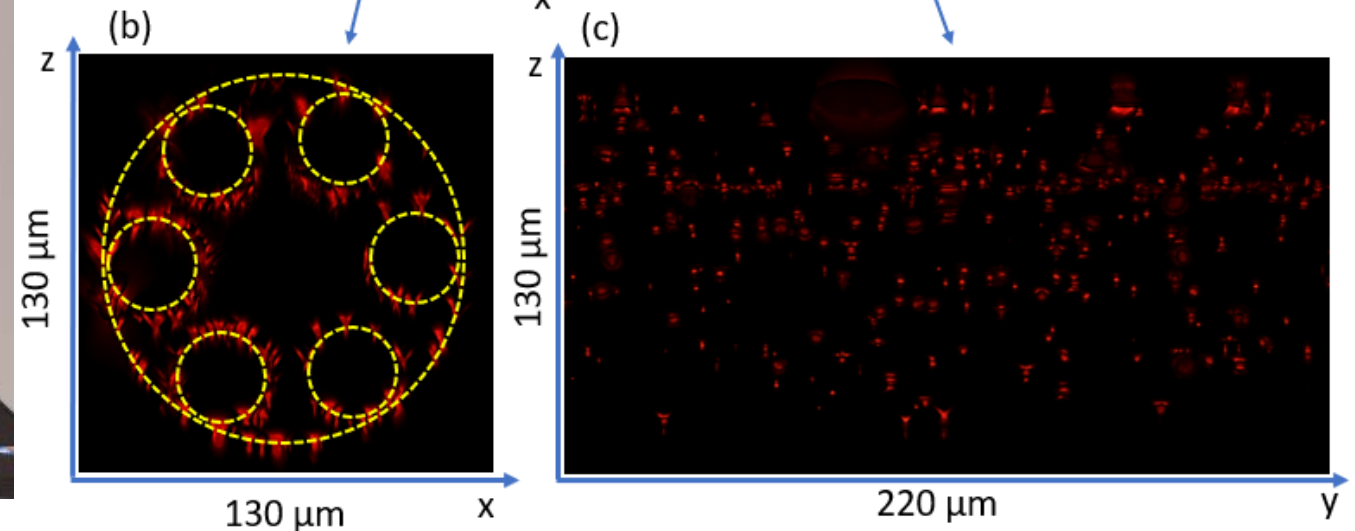
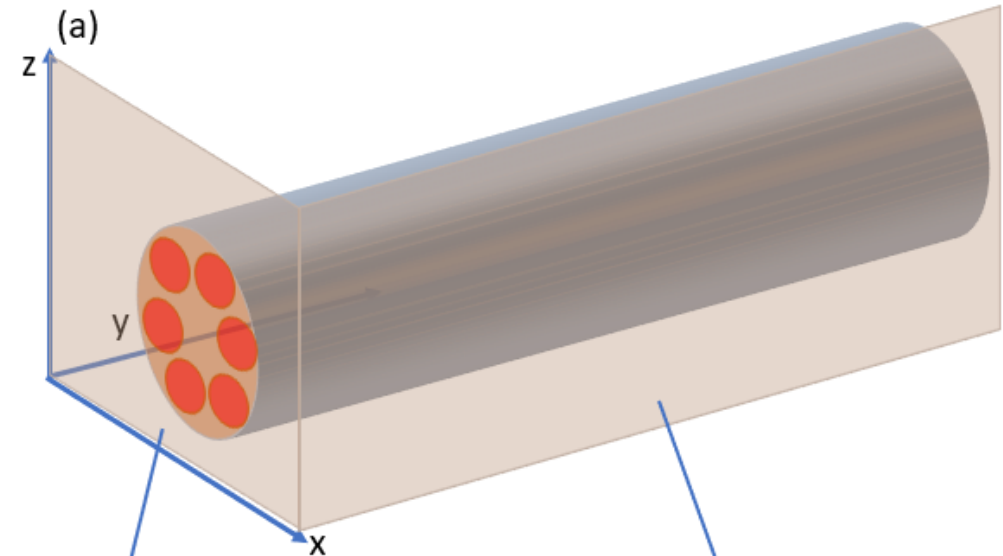


3. Hollow-core anti-resonant fiber

Fiber functionalization and characterization

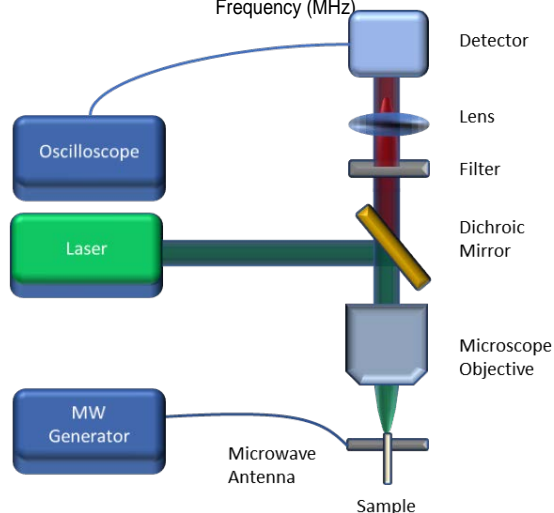
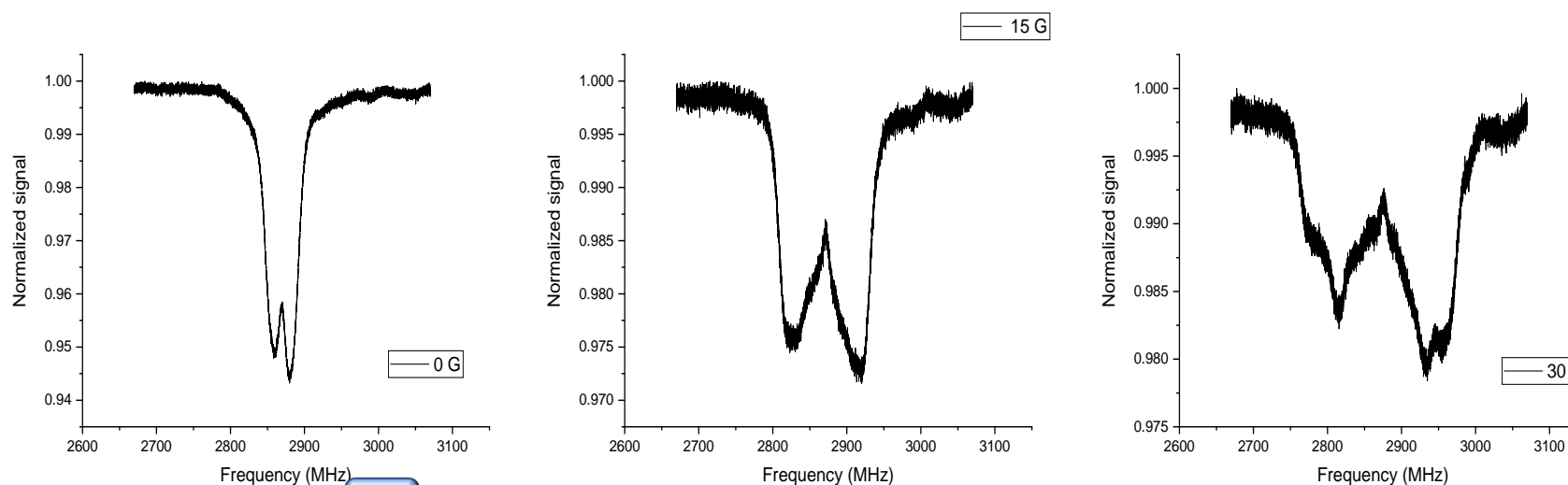
- 40 cm long fiber samples
- Infiltrated with nanodiamond isopropanol (IPA) suspension by a syringe pump
- Flushed with pristine IPA and dried
- Even longitudinal distribution of particles at caldding capillaries

Confocal microscope imaging



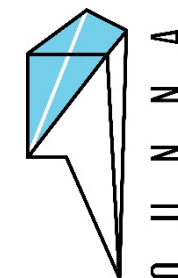
3. Hollow-core anti-resonant fiber

Verification of ODMR magnetic field sensing performance



Basic ODMR performance

- 40 cm long fiber samples
- Confirmed guidance of NV⁻ fluorescence in th hollow core
- **Roughly 15%** readout contrast in face-to-face readout or side readout
- Moderate 1 $\mu\text{T}/\sqrt{\text{Hz}}$ sensitivity



Magnetic field gradiometry

APPLIED PHYSICS LETTERS 113, 011112 (2018)



State of the art in NV nanodiamond vector measurements

- Any random oriented nanodiamond fixation precludes a vector measurement

Alternatives already demonstrated:

- Single crystal vector gradiometer have been on fiber tips
- Dual-core fiber gradiometer with random-oriented ND tip

Quantum stereomagnetometry with a dual-core photonic-crystal fiber

S. M. Blakley,¹ I. V. Fedotov,^{2,3,4} J. Becker,¹ and A. M. Zheltikov^{1,2,3,4,5}

¹Department of Physics and Astronomy, Texas A&M University, College Station, Texas 77843, USA

²Physics Department, International Laser Center, M. V. Lomonosov Moscow State University, Moscow 119992, Russia

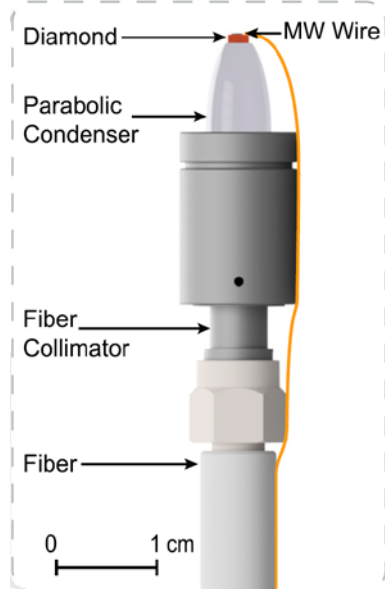
³Russian Quantum Center, ul. Novaya 100, Skolkovo, Moscow 143025, Russia

⁴Kazan Quantum Center, A. N. Tupolev Kazan National Research Technical University, Kazan 420126, Russia

⁵Kurchatov Institute National Research Center, Moscow 123098, Russia

frontiers in Photonics

ORIGINAL RESEARCH
published: 20 August 2021
doi: 10.3389/fphot.2021.732748

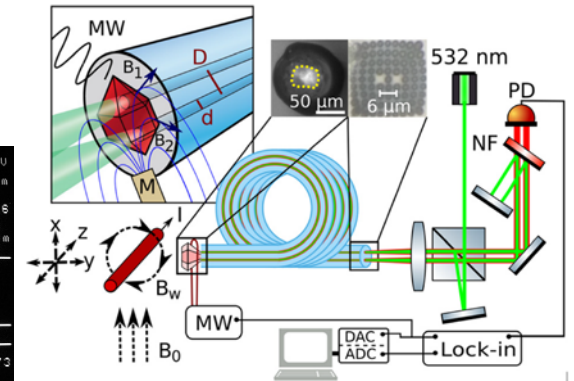
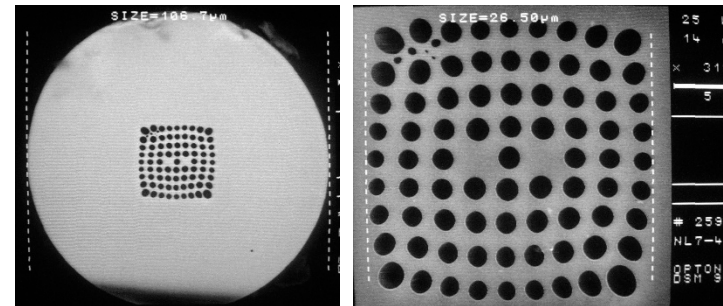


Fiberized Diamond-Based Vector Magnetometers

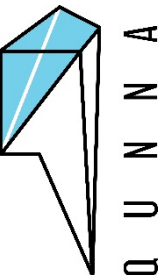
Georgios Chatzidrosos^{1,2*}, Joseph Shaji Rebeiro^{1,2}, Huijie Zheng^{1,2*}, Muhib Omar^{1,2}, Andreas Brenneis³, Felix M. Stürmer³, Tino Fuchs³, Thomas Buck³, Robert Rölver³, Tim Schneemann^{1,2}, Peter Blümler², Dmitry Budker^{1,2,4} and Arne Wickenbrock^{1,2}

¹Helmholtz-Institut, GSI Helmholtzzentrum für Schwerionenforschung, Mainz, Germany, ²Department of Physics, Johannes Gutenberg-Universität Mainz, Mainz, Germany, ³Corporate Sector Research and Advance Engineering, Robert Bosch GmbH, Renningen, Germany, ⁴Department of Physics, University of California, Berkeley, Berkeley, CA, United States

G. Chatzidrosos et al.,
Frontiers in Photonics 2, 732748 (2021)

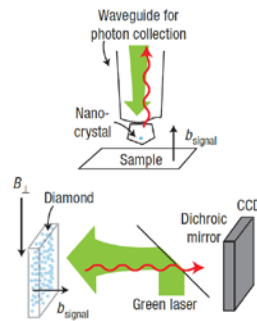


S. M. Blakley et al.,
Appl. Phys. Lett. 113, 011112 (2018)



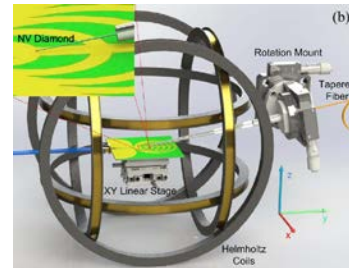
Magnetic field gradiometry - present alternatives employing diamond sensors

Single-crystal diamond-based microscope
Complex but ultra-sensitive

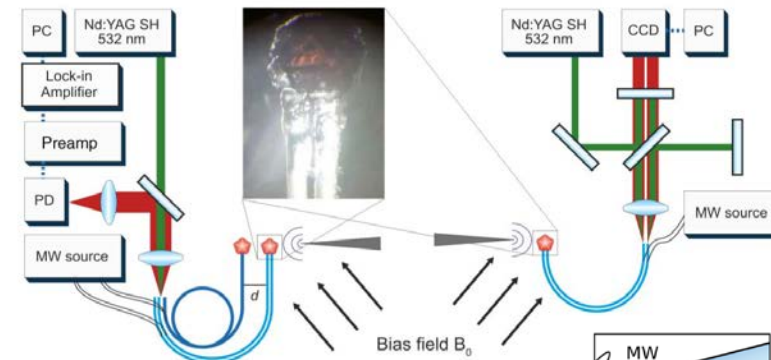


J. M. Taylor et al.,
Nature Physics 4, 810 (2008)

S-C diamond on fiber taper
Robust and sensitive
Requires -preorientation

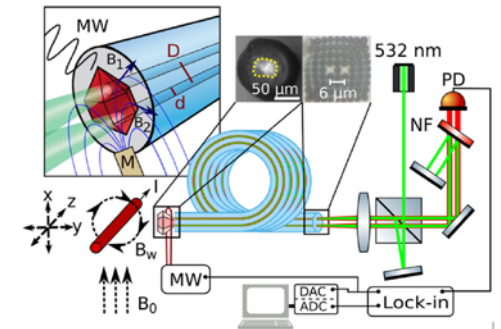


Guo-Bin Chen et al.
IEEE J. Quantum Electron.
56(3), 7500106 (2020)



S. M. Blakley et al.
Opt. Lett. 41(9), 2057 (2016)

Differential gradient measurement
Addressing 1 or 2 diamonds over
two separate fibers or 1 diamond
over a dual core fiber
- Required pre-oriented diamonds



S. M. Blakley et al.
Appl. Phys. Lett. 113, 011112 (2018)

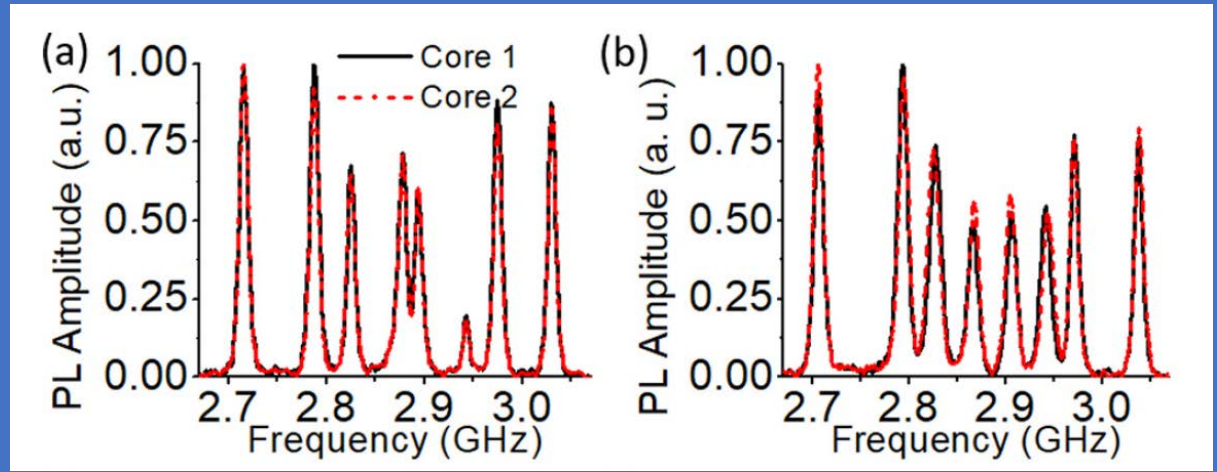
Device simplification

Magnetic field gradiometry - present alternatives

employing

All realizations relied on pre-oriented diamond sensors

for example:

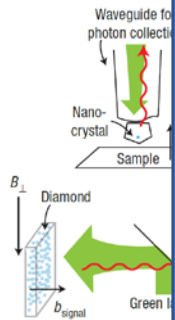


S. M. Blakley et al.
Appl. Phys. Lett. 113, 011112 (2018)

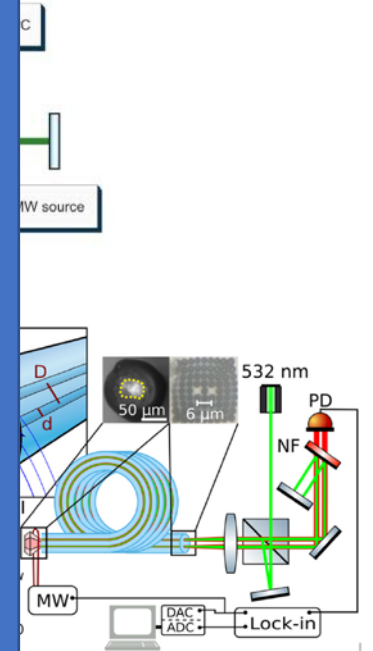
over a dual core fiber
- Required pre-oriented diamonds

S. M. Blakley et al.
Appl. Phys. Lett. 113, 011112 (2018)

Single-crystal diamond
microscope
Complex but ultra

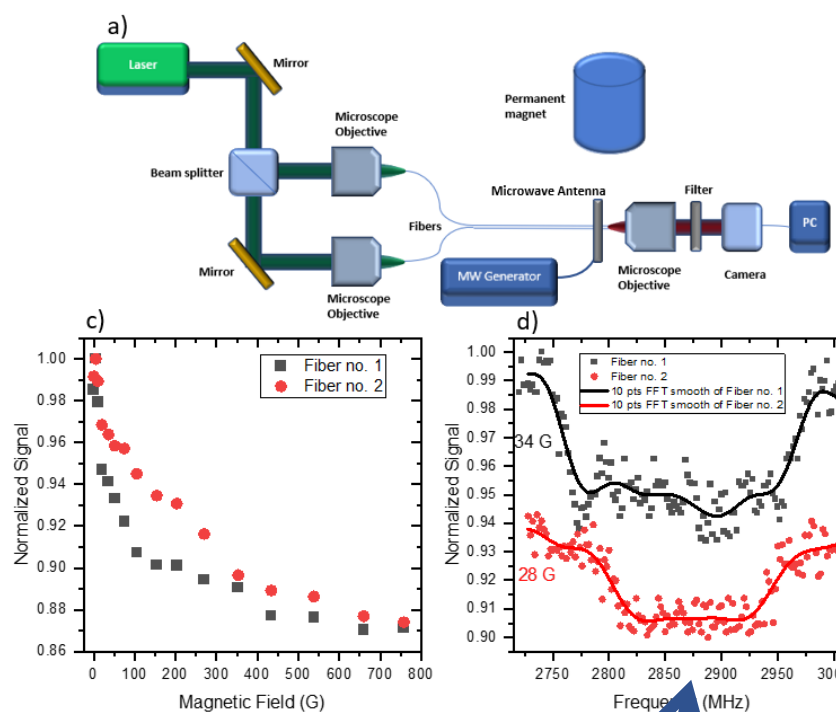
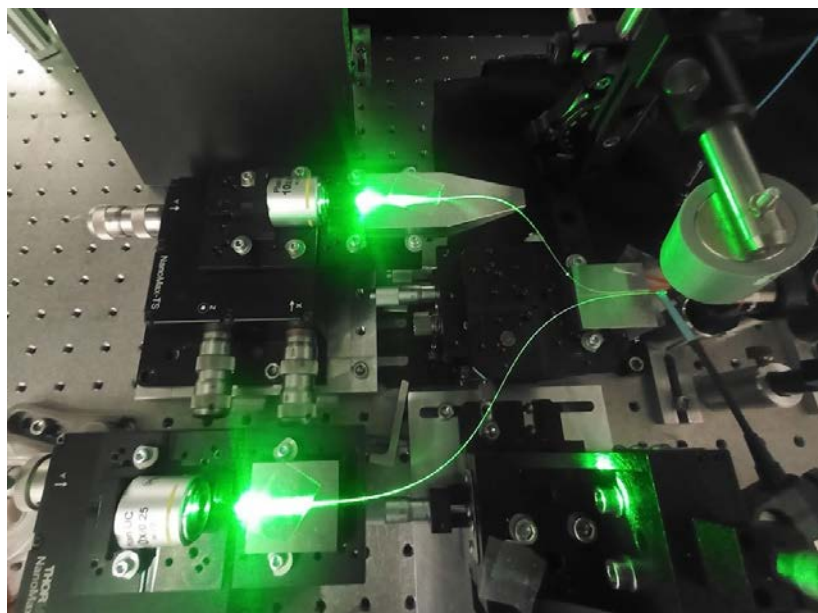


J. M. Taylor et al.
Nature Physics



Device simplification

NV⁻ nanodiamond hollow core fiber proof-of-concept gradiometer



Experimental setup

- Two 40 cm long hollow core fibers with NV⁻ nanodiamonds
- Fiber outputs positions one under-the-other under a magnet
- Removable microwave antenna in place

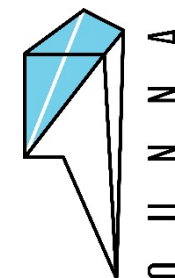
No microwaves variant

- Two experiments
- No-MW variant interesting for big but requires calibration

ODMR variant

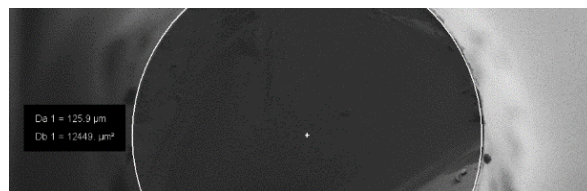
- ODMR variant with 5% relative readout contrast (out of 15% achievable single-fiber ODMR contrast)

Magnetic field gradient obtained despite entirely random diamond orientation

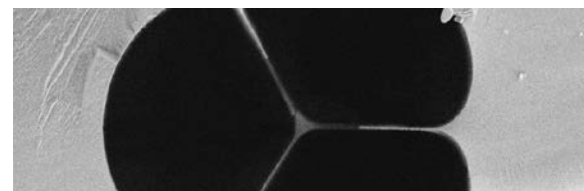


Q
U
N
N
A

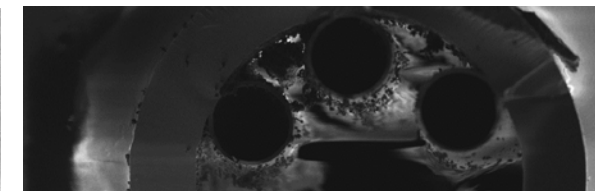
Performance comparison



Step-index multimode fiber



Suspended core fiber

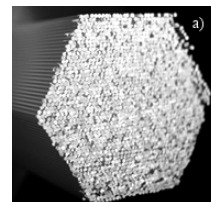


Hollow-core fiber

Material	soft glass (F2) MDNV1um, Adámas Nanotechnologies, in all fibers	soft glass (F2)	fused silica
ODMR readout contrast Direct B-field meas.	3% yes	7% no	15% yes
Sensitivity	$5 \mu\text{T}/\sqrt{\text{Hz}}$	$500 \text{ nT}/\sqrt{\text{Hz}}$	$1 \mu\text{T}/\sqrt{\text{Hz}}$
Usefull fiber length and limiting factor	25 cm scattering	20 cm scattering	40-50 cm infiltration uniformity

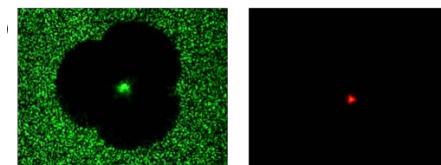
Main advantages

Transverse nanostructure shaping



A. Filipkowski et al. Carbon (2022)

Strong confinement and guiding



A. Filipkowski et al. Opt. Express (2022)

controlled exposure of nanodiamonds

strong NV⁻ signal,
low propagation loss

Optical sytems not optimised – still room for improvement

II. Optical fibers with nanodiamonds: reduction of nonlinearity

Nonlinear refractive index

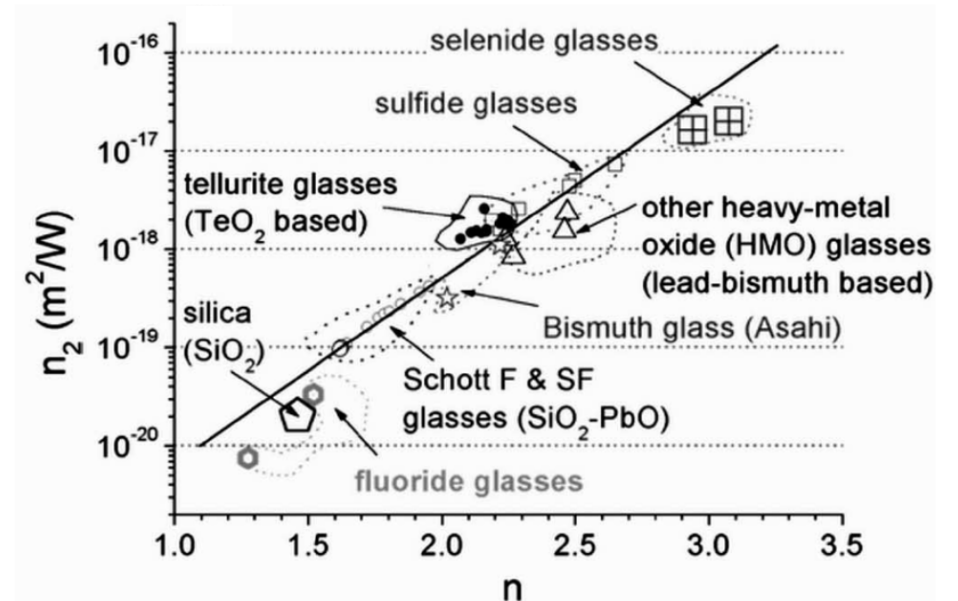
Nonlinearity

material: $n = n_0 + n_2 I_0$

$$n_2 = \frac{3}{4} \frac{\chi^{(3)}}{c \epsilon_0 n_0^2} \quad [\text{m}^2/\text{W}]$$

optical fiber: $\gamma = \frac{2\pi n_2}{A_{eff} \lambda} \quad [1/(\text{W} \cdot \text{km})]$

- electronic response + thermal effects
- nonlinear index of refraction n_2 in the range of 10^{-20} (fused silica, ZBLAN) up to 10^{-17} m^2/W (chalcogenide glass)



X. Feng et. al., *J. Lightwave Technol.* **23**, 2046, (2005).

Negative index of n_2 :

- semiconductors (e.g. GaAs, AlGaAs), strong wavelength dependence, high negative n_2 near to energy gap
- organic liquids
- **nanoparticles** (Au, Ag, diamond), environment-surface effects

Motivation

nonlinear index of refraction n_2

crystalline diamond

$$n_2 = + 4 \div 16 \times 10^{-20} \text{ m}^2/\text{W} \quad [1]$$



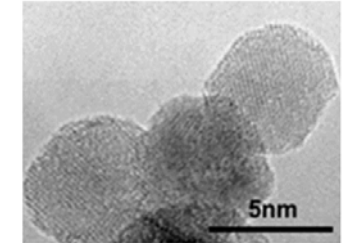
nanodiamonds

$$n_2 = - 2 \times 10^{-17} \text{ m}^2/\text{W} \quad [2]$$

(nanocrystalline membrane, 1 μm)

$$n_2 = - 6 \times 10^{-19} \text{ m}^2/\text{W} \quad [3]$$

(detonation nanodiamond, 5-10 nm)

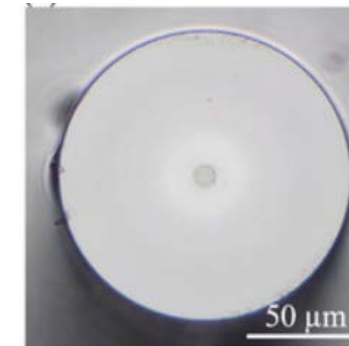


- nanodiamonds:**

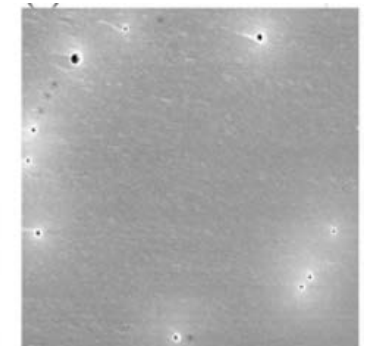
- negative n_2
- size of particles and surface functionalization -> modification of n_2
- successful integration with soft glass (eg. Schott F2) [4]

- GOAL: fiber-drawable hybrid glass with reduced n_2**

- NDs influence on the nonlinearity of hybrid material
- in perspective, fiber optics with zero nonlinearity



Ref [4]



[1] J.M.P. Almeida et. al., „Nonlinear optical spectrum of diamond at femtosecond regime”, *Sci. Rep.* **7**, 2017

[2] F. Trojáněk et. al., „Nonlinear optical properties of nanocrystalline diamond”, *Opt. Express* **18**(2), 2010

[3] O. Muller et. al., „Optical limiting properties of surface functionalized nanodiamonds probed by the Z-scan method”, *Sci. Rep.* **9**, 2019

[4] D. Bai et al., „Fluorescent diamond microparticle doped glass fiber for magnetic field sensing,” *APL Materials* **8**, 081102 (2020)

Measuring method – Z-scan

- nonlinear phase change at the beam waist (self-focusing $n_2 > 0$, self-defocusing $n_2 < 0$)

$$\Delta\phi = \frac{2\pi}{\lambda} n_2 I_0 L_{eff} \quad I_0 = \frac{2P_0}{\pi\omega_0^2} \quad L_{eff} = \frac{(1 - e^{-\alpha L})}{\alpha}$$

L - sample thickness

ω_0 - beam waist at the focus (radius)

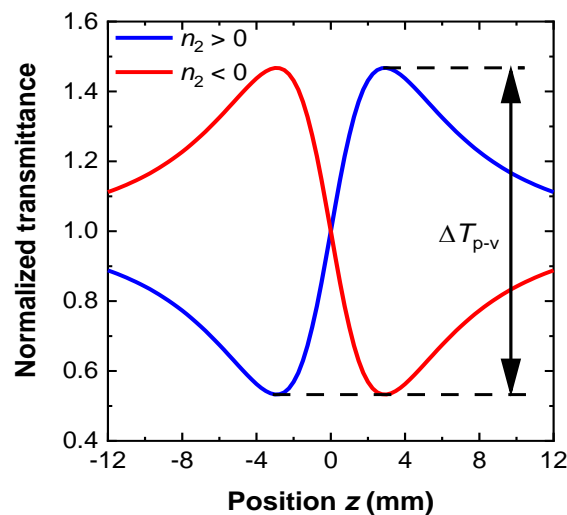
α - linear absorption coefficient

P_0 - peak power

- normalized transmittance (closed aperture)

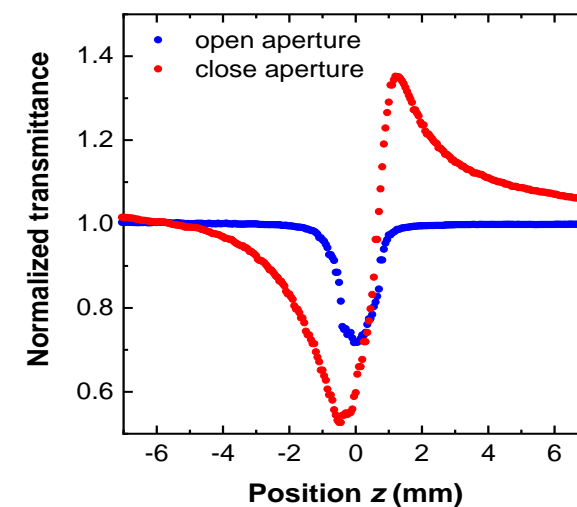
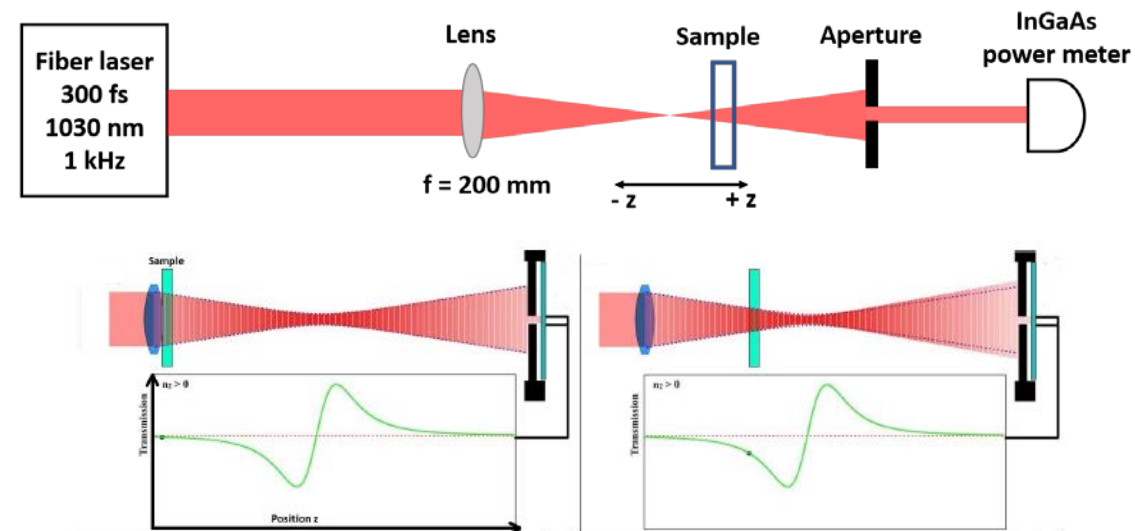
$$T(z, \Delta\Phi_0) = 1 - \frac{4x\Delta\Phi_0}{(x^2+1)(x^2+9)} \quad x = z/z_0$$

z_0 - Rayleigh range



- closed aperture → nonlinear refraction n_2
- open aperture → nonlinear absorption β

M. Sheik-Bahae et. al. , "Sensitive measurement of optical nonlinearities using a single beam," *IEEE J. Quantum Electron.* **26** (4), 760-769 (1990)



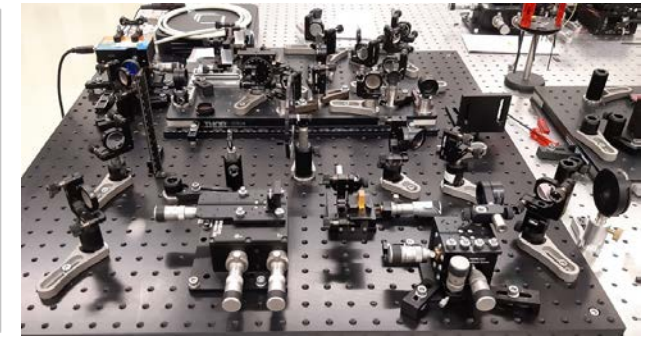
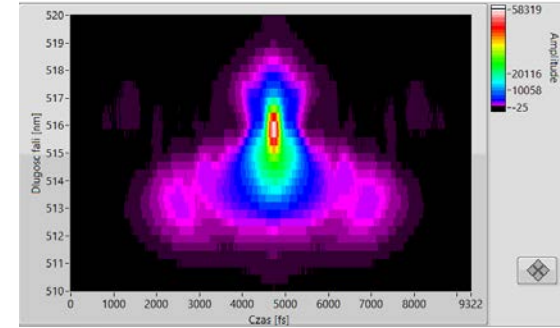
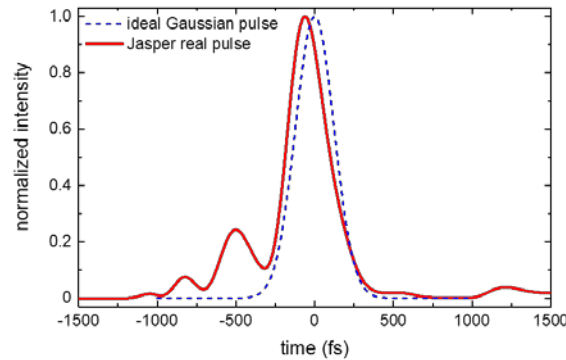
Z-scan, system parameters

- laser pulse characterization (Frequency Resolved Optical Gating - FROG)

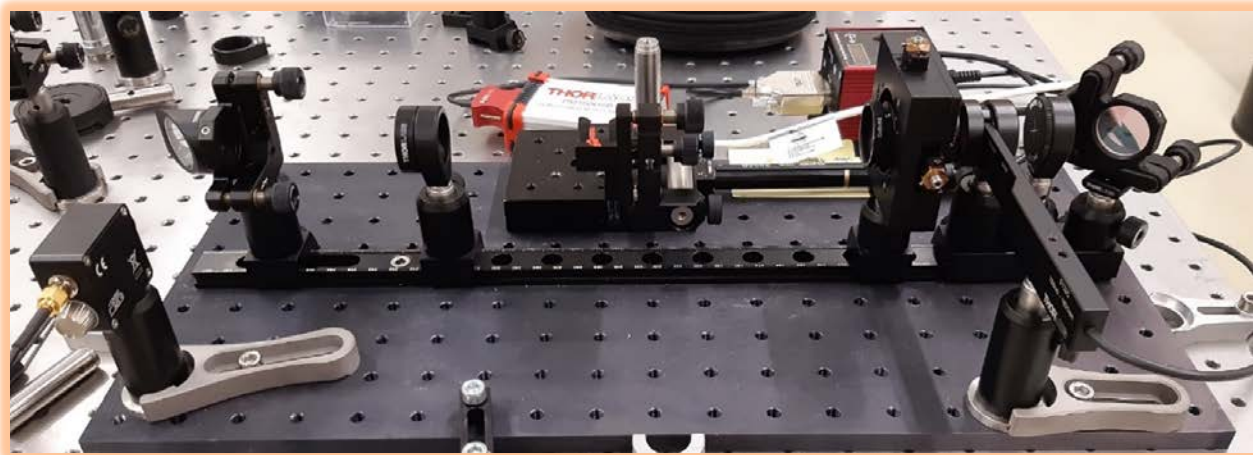
Fluence Jasper X0
(1030 nm, 300 fs, 1 kHz)

peak power scaling factor

$$\frac{P_{real}}{P_{Gauss}} \approx 0.8$$



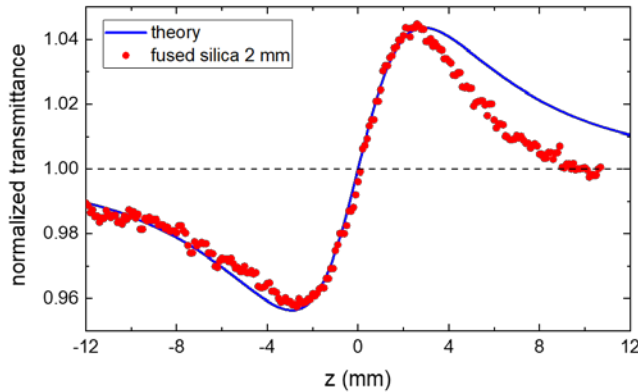
- portable Z-scan setup



- plano-convex lens $f = 200$ mm
- beam parameters: $M^2 < 1.2$, $\omega_0 = 37$ μm , $z_0 = 4.2$ mm
- beam diameter at scanning boundaries: 230 μm
- low power measurement for liquids
($P_{avg} = 2.27$ mW, $E_p = 2.2$ μJ , $I_0 = 240$ GW/cm²)
- travel range 24 mm
- InGaAs power meter (700 \div 1800 nm)

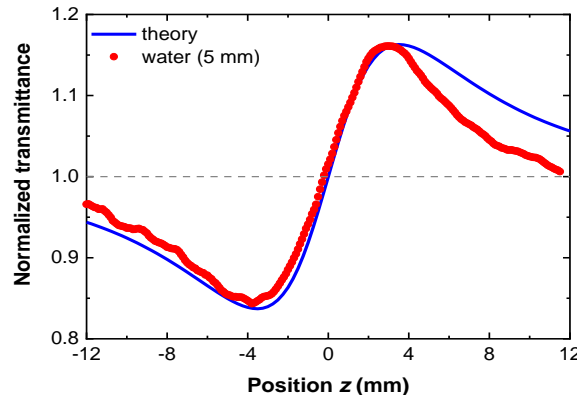
System check

- reference fused silica sample (2 mm)



$2.1 - 2.3 \times 10^{-20} \text{ m}^2/\text{W}$

- distilled water in quartz cuvette (5 mm)



$3.27 \times 10^{-20} \text{ m}^2/\text{W}$

Ref. [1], for 300 fs
 $3.35 \times 10^{-20} \text{ m}^2/\text{W}$

- toluene in quartz cuvette (5 mm) $17 \times 10^{-20} \text{ m}^2/\text{W}$

- results for reference samples (thin and thick sample assumption)

sample	sample thickness	lens	n_2	n_2 [Ref]
Fused silica	2 mm	50 mm ($Z_0 = 0.86 \text{ mm}$)	1.8 – thin sample 2.1 – thick sample	2.24 (1.7 – 2.7)
	2 mm	100 mm ($Z_0 = 3.44 \text{ mm}$)	2.1 – thin sample 2.2 – thick sample	
	5 mm	100 mm ($Z_0 = 3.44 \text{ mm}$)	2.2 – thin sample 2.1 – thick sample	
Schott F2	2 mm	50 mm ($Z_0 = 0.86 \text{ mm}$)	5.0 – thin sample 5.7 – thick sample	2.9 8.9
	2 mm	100 mm ($Z_0 = 3.44 \text{ mm}$)	6.9 – thin sample 7.0 – thick sample	
YVO4	0.9 mm	50 mm ($Z_0 = 0.86 \text{ mm}$)	18.6 (pol1), 18.3 (pol2)	15 - 19

$n_2 \times 10^{-20} \text{ m}^2/\text{W}$

[1] M. L. Miguez et. al., "Measurement of third-order nonlinearities in selected solvents as a function of the pulse width," *Opt. Express* **25**, 3553-3565 (2017)

Nanodiamond in water

- Why water?

low n_2 and dense enough to avoid settling down

isopropanol? Quick particles settling -> unrepeatable scans

DMSO? Very stable suspension but high n_2 (NDs don't change n_2 of suspension)

- samples:

1. detonation nanodiamonds (DND; Adámas Nanotechnologies, dominant particles size 5-10 nm), concentration of **0.01 mg/ml**

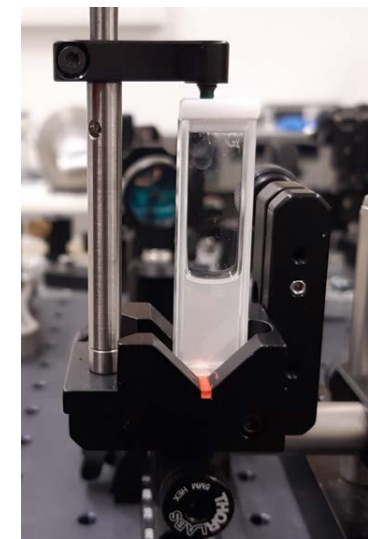
2. DND concentration of **0.1 mg/ml**

3. monocrystalline synthetic nanodiamonds (MSY, Pureon, average size 250 nm), concentration of **0.01 mg/ml**

- preparation:

1. mechanical shaking + 1h in ultrasonic cleaner

2. measurement in quartz cuvette (1 mm wall thickness and 5 mm optical path)

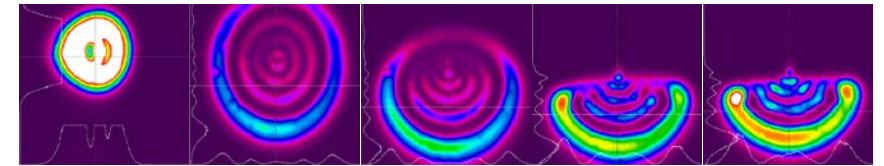
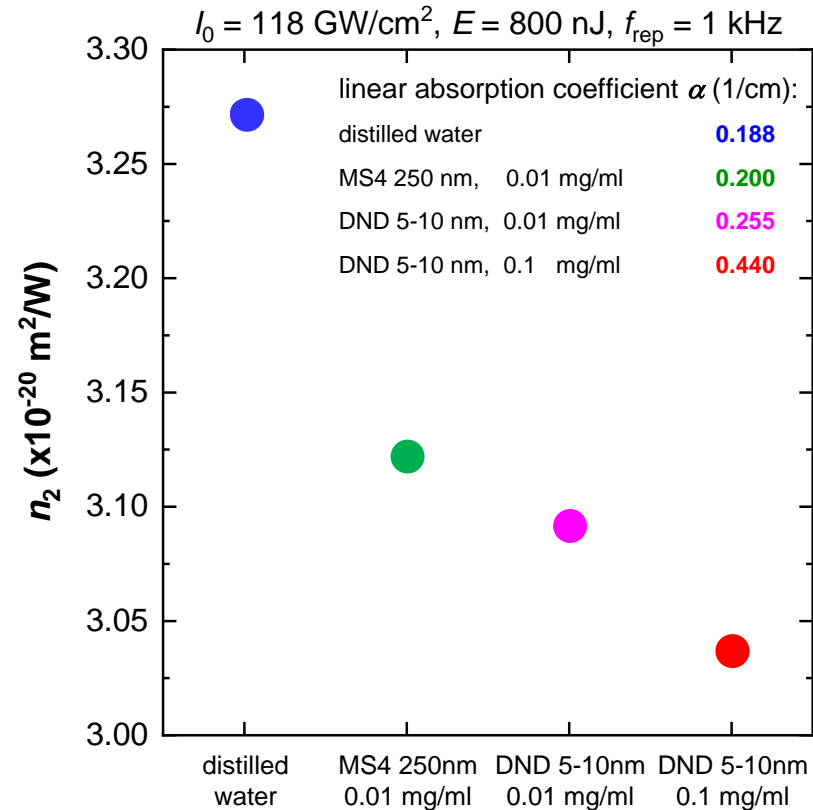
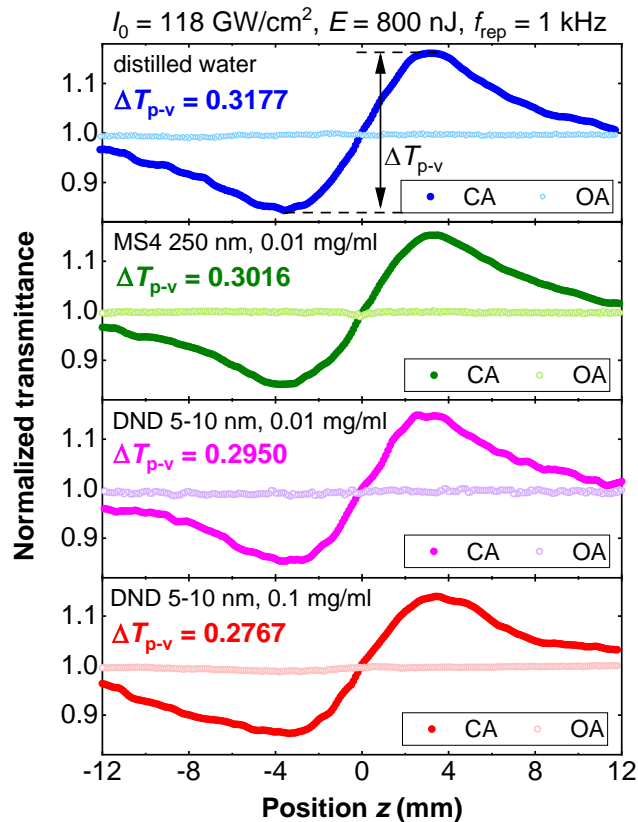


- absorption coefficient α
reflection from 4 surfaces included

$$\alpha = -\frac{1}{L} \ln \left(\frac{P_{out}}{P_{in}(T_1 T_2)^2} \right)$$

Nanodiamond in water

- requirements for the selective measurement of electronic response in liquids: **short pulses (< ps)** and **low repetition rate (< 1 kHz)**
- long pulses or high repetition rate -> **thermal lensing** -> (spatial self-phase modulation)



- α rises for higher concentration of NDs -> scattering
- small particles -> lower n_2
- high concentration -> lower n_2
- distilled water: $n_2 = 3.27 \times 10^{-20} \text{ m}^2/\text{W}$
- DND 0.1 mg/ml: $n_2 = 3.04 \times 10^{-20} \text{ m}^2/\text{W}$
- up to **7%** of n_2 reduction for DND 0.1 mg/ml

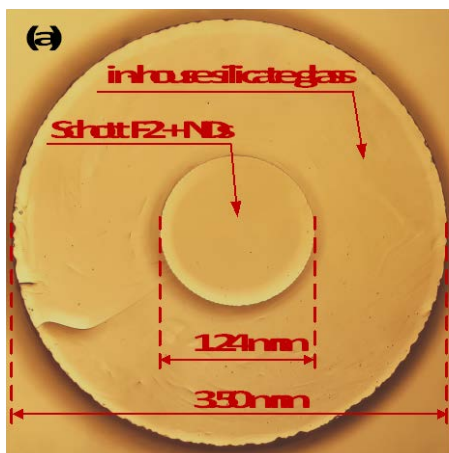
Bulk F2 glass with NDs - fabrication

- materials:

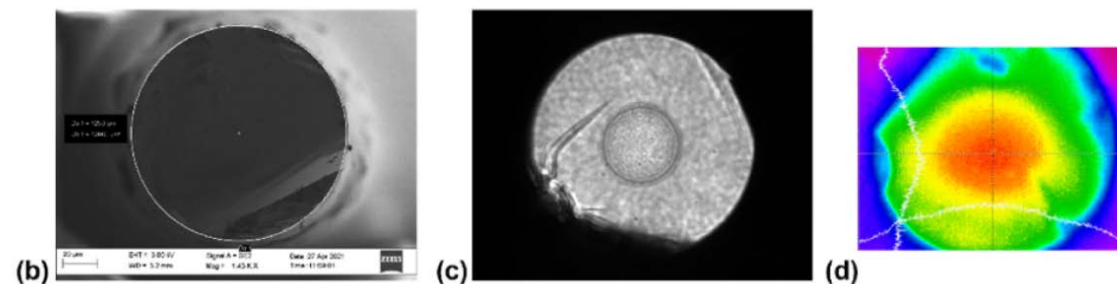
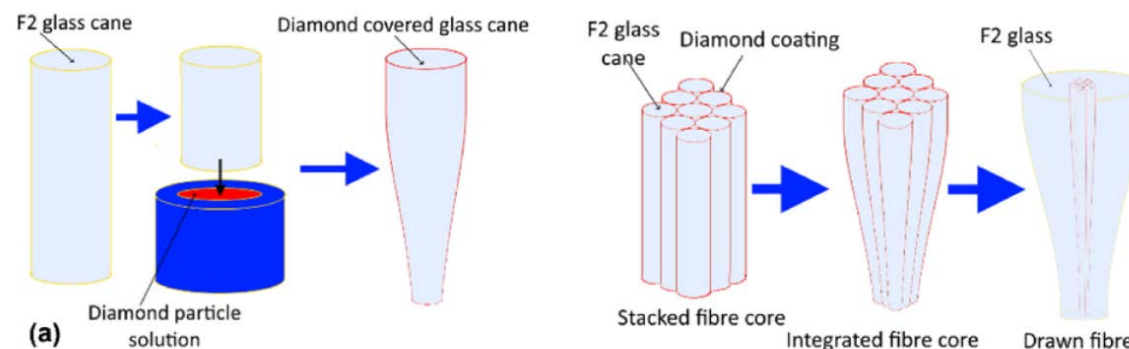
- lead-silicate glass rods (Schott F2), $n_d = 1.6199$
- nanodiamonds (MDNV, Adamas Nanotechnologies, 750 nm) suspended in isopropanol
- modified in-house developed F2 glass with lower RI, $n_d = 1.6133$

- dip-coating + stack-and-draw method:

- Schott F2 rods immersed in ND + IPA (10 x)
- drawing the canes
- core stacking (**790 rods covered with NDs**) and drawing
- preform fabrication: core inside the modified F2 tube



sample of the preform
thickness 2 mm

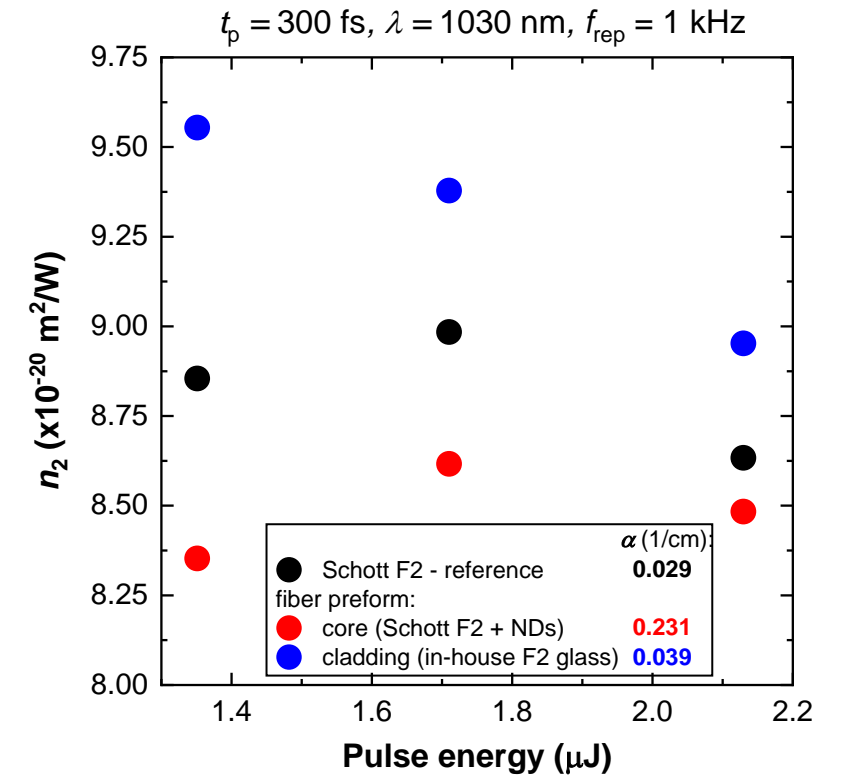
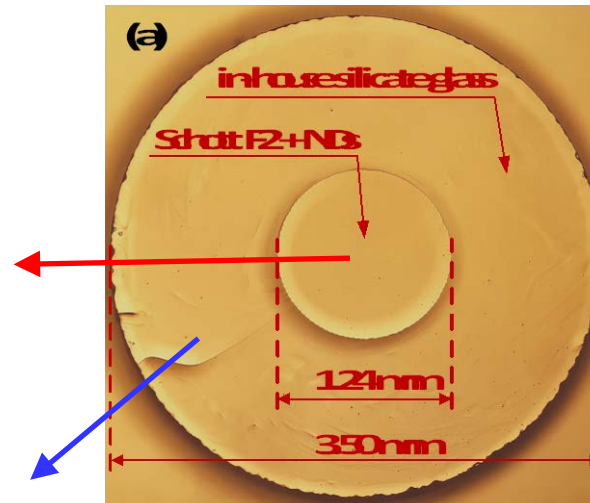
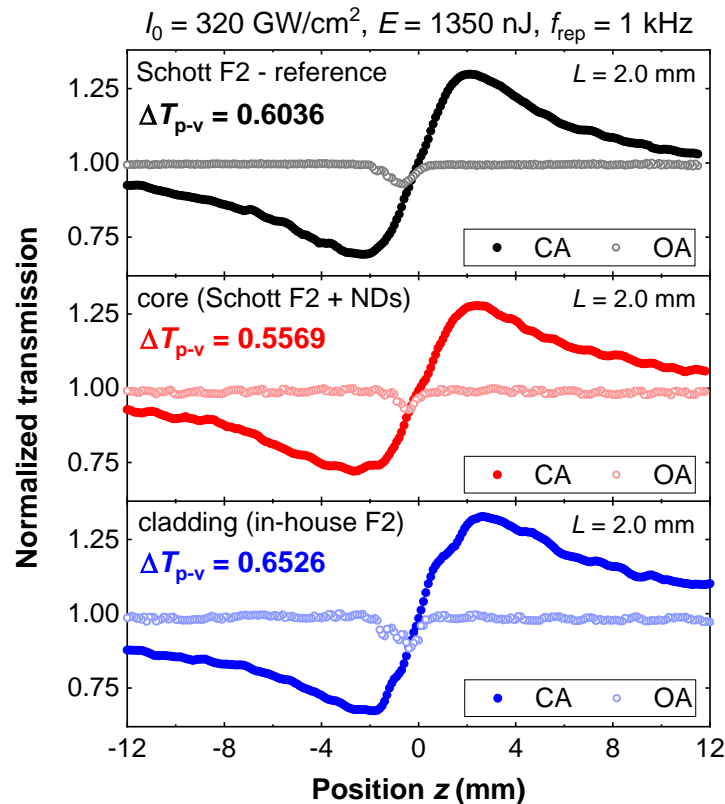


A. Filipkowski, et al., "Volumetric incorporation of NV diamond emitters in nanostructured F2 glass magneto-optical fiber probes," *Carbon* 196, 10-19, (2022).

Bulk F2 glass with NDs - nonlinearity

- Z-scan measurement of:
 - core -> Schott F2 + NDs
 - cladding -> modified F2 glass
 - reference Schott F2 glass sample, thickness 2 mm

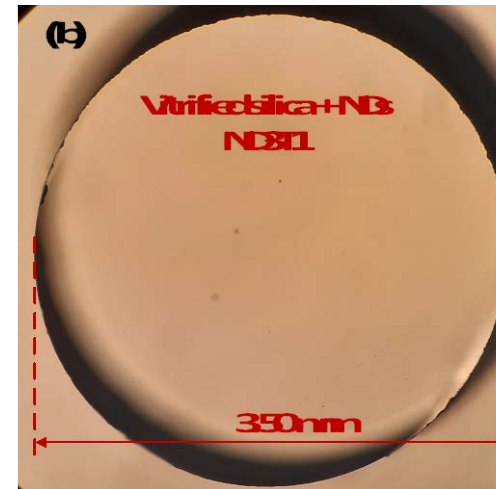
- 10x higher α in the core (scattering)
- 4% - 7% of n_2 reduction for F2 + NDs glass



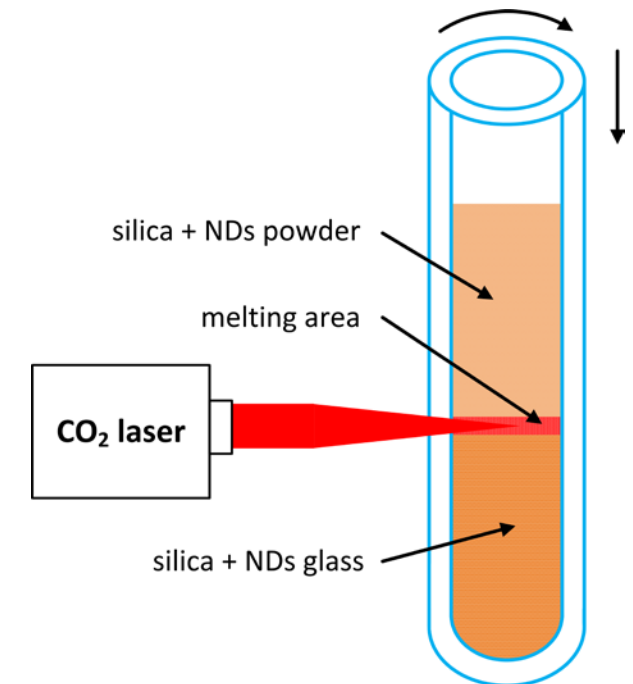
Vitrified silica glass with NDs - fabrication

- materials:
 - detonation nanodiamonds (DND 180 nm) mixed with silica powder in ethanol (10 µg DND per 1 g of silica)
 - silica tube
- CO₂ laser vitrification process
 - DND + silica mixture drying
 - heating DND + silica powder in silica tube (600°C)
 - laser vitrification along the capillary with powder
 - not uniform preforms due to process modification

two-sided polished sample of the preform
thickness 2 mm



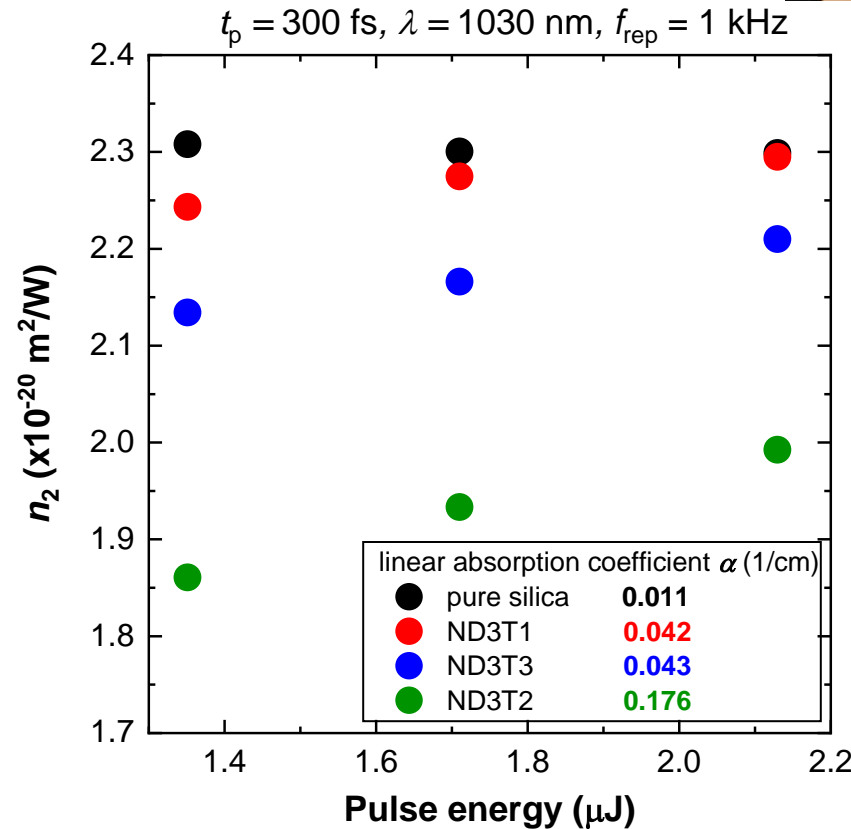
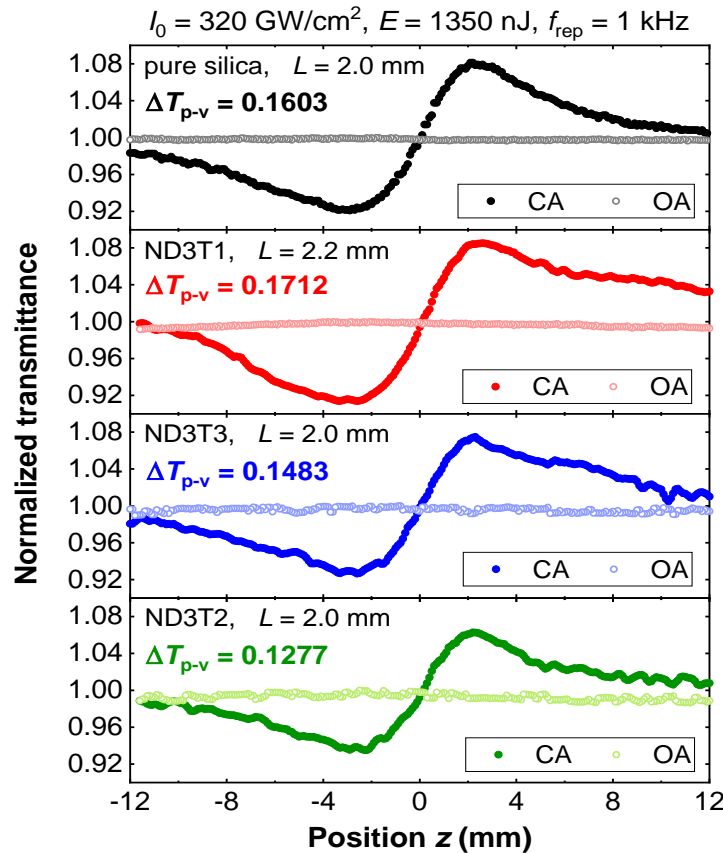
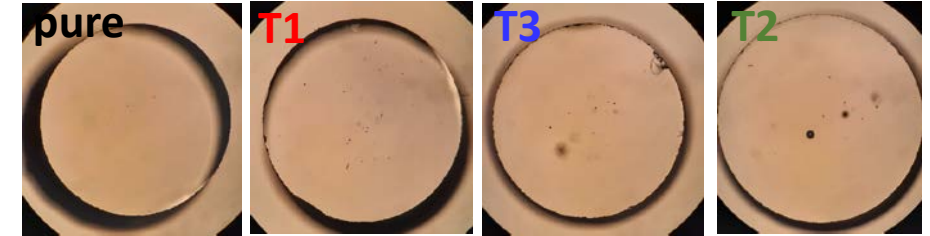
Prof. Alex Heidt



Vitrified silica glass with NDs - nonlinearity

- Z-scan measurement of:

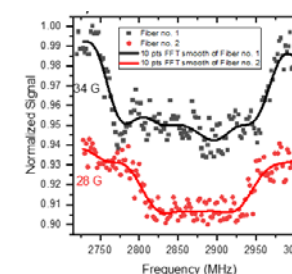
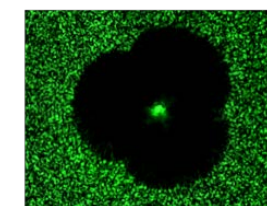
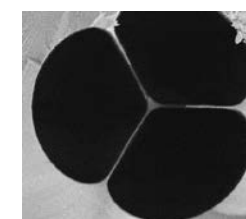
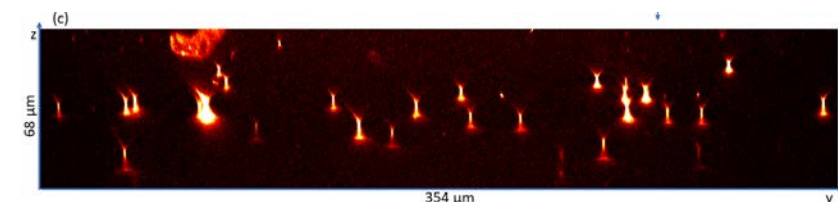
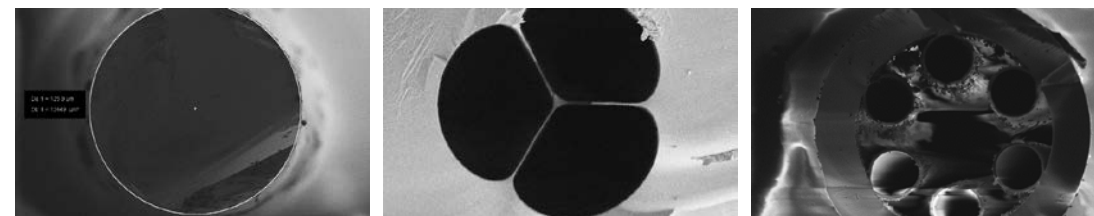
- vitrified pure silica glass
- vitrified silica glass with NDs (samples ND3T1-3)



- vitrified silica has the same n_2 as commercial fiber grade silica glass
- all samples with NDs have higher α and lower n_2 than pure silica
- possibly inhomogeneous ND dopant
- 13% - 19% of n_2 reduction for ND3T2 sample**

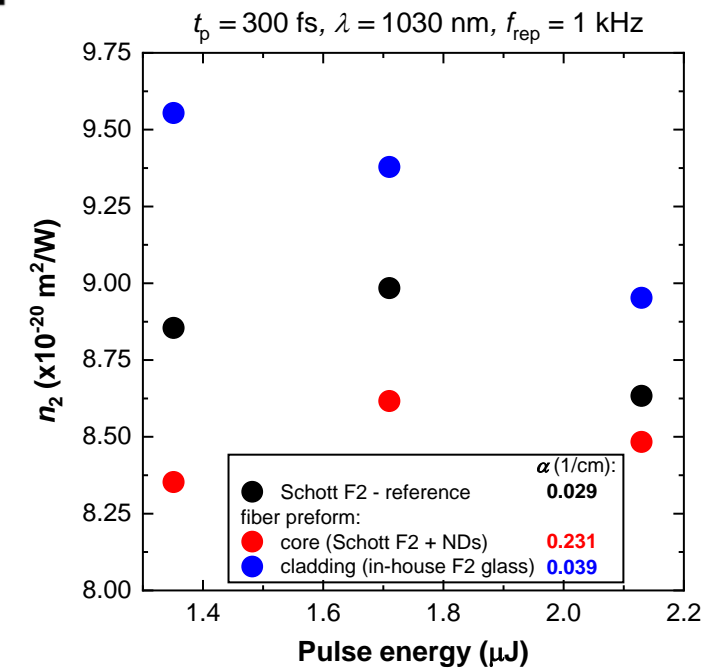
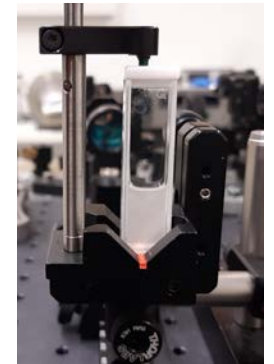
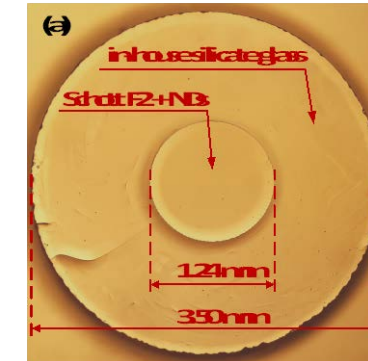
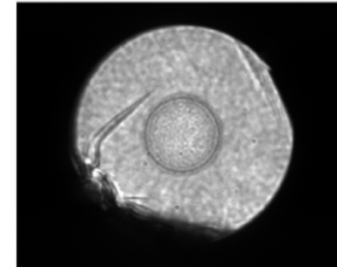
Conclusions 1/2

- Volumetric functionalization of optical fibers with nanodiamonds enables practical magnetic field sensors across different fiber geometries
- Modified stack-and-draw fiber development enables control of diamond particle distribution at the micro-scale
- Diamond's NV fluorescence can be effectively captured and guided in strongly confining fibers
- Magnetic field gradient information is obtainable using randomly oriented spins in nanodiamond - towards vector measurements?



Conclusions 2/2

- Nanodiamonds decrease nonlinear index of refraction in all examined host materials:
 - water **4.5% ÷ 7.0%** (0.8 μJ)
 - Schott F2 glass **4.2 %** (1.7 μJ)
 - vitrified silica glass **1.0 % ÷ 16%** (1.7 μJ)
- Fabricated hybrid glass with NDs are useful for optical fiber development
- Nonlinearity can be controlled by NDs particle size, surface functionalization and concentration
- Further reduction of n_2 may result high loss (a zero nonlinear fiber can be a challenge)



ACKNOWLEDGEMENTS



TEAM NET Programme POIR.04.04.00-00-1644/18